

Genes and sites under adaptation at the phylogenetic scale also exhibit adaptation at the population-genetic scale

T. Latrille^{1,2,3}, N. Rodrigue⁴, N. Lartillot¹

¹Université de Lyon, Université Lyon 1, CNRS, VetAgro Sup, Laboratoire de Biométrie et Biologie Evolutive, UMR5558, Villeurbanne, France

²École Normale Supérieure de Lyon, Université de Lyon, Lyon, France

³Department of Computational Biology, Université de Lausanne, Lausanne, Switzerland

⁴Department of Biology, Institute of Biochemistry, and School of Mathematics and Statistics, Carleton University, Ottawa, Canada

thibault.latrille@ens-lyon.org

Supplementary materials

Contents

1	Running Bayescode	2
1.1	Site-specific ω -based codon models	2
1.2	Site-specific mutation-selection codon models	2
2	Gene ontology enrichment at gene and site level	3
2.1	Gene-specific mutation-selection model	3
2.2	Site-specific ω -based model	4
2.3	Site-specific mutation-selection model	5
2.4	Exclusive to site-specific mutation-selection model	7
3	Graphical abstract for the pipeline.	9
4	Rate of adaptation enrichment while controlling for ω	10
4.1	Mutation-selection codon model at gene level ($\alpha = 0.05$)	11
4.2	Mutation-selection codon model at site level ($\alpha = 0.05$)	13
5	Rate of adaptation enrichment with $\alpha = 0.005$	15
5.1	Scatterplot with $\alpha = 0.005$	15
5.2	Mutation-selection codon model at gene level ($\alpha = 0.005$)	16
5.3	Mutation-selection codon model at site level ($\alpha = 0.005$)	17
6	Rate of adaptation enrichment with polyDFE	18
6.1	PolyDFE model C - including divergence data	18
6.2	PolyDFE model C - polymorphism data alone with $\beta > 0$	21
6.3	PolyDFE model C - polymorphism data alone with $\beta > 5$	23
6.4	PolyDFE model D - including divergence	25
7	References	28

1 Running Bayescode

1.1 Site-specific ω -based codon models.

The 61-by-61 codon substitution matrix ($\mathbf{q}^{(i)}$) at site i is defined entirely by the mutation matrix ($\boldsymbol{\mu}$), $\omega^{(i)}$ and the genetic code:

$$\begin{cases} q_{a \rightarrow b}^{(i)} = 0 & \text{if codons } a \text{ and } b \text{ are more than one mutation away,} \\ q_{a \rightarrow b}^{(i)} = \mu_{a \rightarrow b} & \text{if codons } a \text{ and } b \text{ are synonymous,} \\ q_{a \rightarrow b}^{(i)} = \omega^{(i)} \mu_{a \rightarrow b} & \text{if codons } a \text{ and } b \text{ are non-synonymous.} \end{cases} \quad (1)$$

By definition of the instantaneous rate matrix, the sum of the entries in each row of the codon substitution rate matrix \mathbf{q} is equal to 0, giving the diagonal entries:

$$q_{a \rightarrow a}^{(i)} = - \sum_{b \neq a, b=1}^{61} q_{a \rightarrow b}^{(i)}. \quad (2)$$

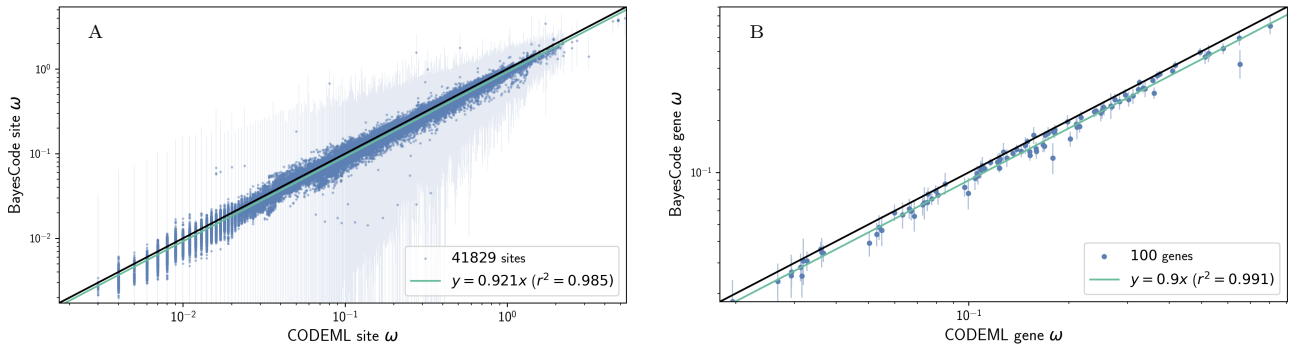
In *BayesCode* (<https://github.com/ThibaultLatrille/BayesCode>), ω -based site-specific codon models are obtained by running *mutselomega* with the options:

```
mutselomega --omegashift 0.0 --freeomega --omegancat 30 --flatfitness -a my_alignment.phy -t my_tree.newick -u 2000 my_genename
```

The mean value of ω per site is then obtained by running *readmutselomega* with the options:

```
readmutselomega --every 1 --until 2000 --burnin 1000 -c 0.025 my_genename
```

Figure S1:



Panel A: site-specific ω posterior mean as given by *BayesCode* (y-axis) with 95% posterior credibility intervals (light blue) as a function of ω estimates given by CODEML (x-axis) for 41,829 sites across 100 random genes. Panel B: gene-specific ω posterior mean as given by *BayesCode* (y-axis) with 95% posterior credibility intervals as a function of ω estimates given by CODEML (x-axis) for 100 random genes. Linear regression is shown in the green solid line, and the identity ($y=x$) in black solid line.

1.2 Site-specific mutation-selection codon models

In *BayesCode* (<https://github.com/ThibaultLatrille/bayescode>), mutation-selection codon models are obtained by running *mutselomega* for 2000 points of MCMC with the options:

```
mutselomega ---omegashift 0.0 --ncat 30 -a my_alignment.phy -t my_tree.newick -u 2000 my_genename
```

The collection of site-specific fitness profiles ($\mathbf{F}^{(i)}, \forall i$) are then obtained by running *readmutselomega*, reading 1000 points of MCMC (first 1000 are considered as burn-in) with the options:

```
readmutselomega --every 1 --until 2000 --burnin 1000 --ss my_genename
```

The gene-specific mutation matrix ($\boldsymbol{\mu}$) is also obtained by running *readmutselomega*, reading 1000 points of MCMC (first 1000 are considered as burn-in) with the options:

```
readmutselomega --every 1 --until 2000 --burnin 1000 --nuc my_genename
```

2 Gene ontology enrichment at gene and site level

2.1 Gene-specific mutation-selection model

Genes are classified under an adaptive regime if the lower bound for the posterior credibility interval of gene-specific ω ($\alpha = 0.05$) is above the upper bound of the posterior credibility interval of gene-specific ω_0 . Because this is a unilateral test ($\omega > \omega_0$) and the two posterior credibility interval are independent, the risk is $(\alpha/2)^2 = 0.025^2 = 6.25 \times 10^{-4}$ for each gene. Genes are classified as control if they are not in the adaptive group. For each ontology (775 ontologies), a 2x2 contingency tables is built by counting the number of genes based on their evolutionary regime (adaptive regime or control group) and their ontology (whether they have this specific ontology or not). Fisher's exact tests are then performed for these 2x2 contingency tables. p_v^{adj} are corrected for multiple comparison (Holm-Bonferroni correction).

Table S1: Ontology enrichment with gene-specific mutation-selection model

Gene ontology	n_{Observed}	n_{Expected}	Odds ratio	p_v	p_v^{adj} (* if < 0.05)
immune system process	48	5.625	8.533	9.8×10^{-24}	7.6×10^{-21}*
extracellular space	82	19.8	4.151	6.2×10^{-21}	4.8×10^{-18}*
innate immune response	41	5.245	7.817	1.6×10^{-19}	1.2×10^{-16}*
extracellular region	99	30.5	3.251	5×10^{-18}	3.9×10^{-15}*
regulation of complement activation	14	0.359	39.0	1.2×10^{-13}	9.4×10^{-11}*
extracellular exosome	100	38.2	2.618	3.6×10^{-13}	2.7×10^{-10}*
complement activation	12	0.180	66.6	5.3×10^{-13}	4×10^{-10}*
immune response	28	4.054	6.907	6.5×10^{-13}	5×10^{-10}*
blood microparticle	17	1.247	13.6	7.1×10^{-12}	5.5×10^{-9}*
serine-type endopeptidase activity	20	2.243	8.917	3.1×10^{-11}	2.4×10^{-8}*
inflammatory response	27	5.129	5.264	2.5×10^{-10}	1.9×10^{-7}*
integral component of membrane	149	78.4	1.901	1.4×10^{-8}	1.1×10^{-5}*
defense response to virus	15	1.795	8.355	1.7×10^{-8}	1.3×10^{-5}*
complement activation	8	0.182	43.9	1.8×10^{-8}	1.4×10^{-5}*
integral component of plasma membrane	58	23.0	2.516	2×10^{-8}	1.5×10^{-5}*
leukocyte migration	16	2.210	7.239	2.8×10^{-8}	2.1×10^{-5}*
neutrophil degranulation	28	7.432	3.767	6×10^{-8}	4.5×10^{-5}*
external side of plasma membrane	18	3.156	5.703	7.6×10^{-8}	5.7×10^{-5}*
plasma membrane	131	70.7	1.852	1.2×10^{-7}	9.1×10^{-5}*
lipid metabolic process	31	9.452	3.280	1.9×10^{-7}	0.00014*
proteolysis	34	11.2	3.047	2.4×10^{-7}	0.00018*
platelet degranulation	14	1.982	7.064	2.5×10^{-7}	0.00019*
cell surface	29	9.210	3.149	9.1×10^{-7}	0.00069*
extracellular vesicle	10	0.969	10.3	9.5×10^{-7}	0.00072*
serine-type peptidase activity	13	1.927	6.746	1×10^{-6}	0.00076*
toll-like receptor signaling pathway	9	0.729	12.4	1.1×10^{-6}	0.00086*
chemotaxis	13	1.988	6.540	1.3×10^{-6}	0.001*
defense response to bacterium	12	1.690	7.100	1.7×10^{-6}	0.001*
adaptive immune response	13	2.048	6.347	1.7×10^{-6}	0.001*
cilium movement	7	0.366	19.1	2.8×10^{-6}	0.002*
apical plasma membrane	21	5.830	3.602	4.2×10^{-6}	0.003*
chemokine-mediated signaling pathway	7	0.488	14.3	9.5×10^{-6}	0.007*
cell surface receptor signaling pathway	18	4.787	3.760	1.2×10^{-5}	0.009*
cytolysis	5	0.123	40.8	1.3×10^{-5}	0.009*
antimicrobial humoral response	5	0.123	40.8	1.3×10^{-5}	0.009*
positive regulation of heterotypic cell-cell adhesion	5	0.123	40.8	1.3×10^{-5}	0.009*
hemostasis	9	1.094	8.225	1.3×10^{-5}	0.010*
cellular protein metabolic process	14	3.134	4.468	2×10^{-5}	0.015*
positive regulation of ERK1 and ERK2 cascade	14	3.194	4.383	2.5×10^{-5}	0.018*
platelet alpha granule	5	0.184	27.2	3.2×10^{-5}	0.024*
dynein light chain binding	5	0.184	27.2	3.2×10^{-5}	0.024*
lysosome	21	7.167	2.930	6.1×10^{-5}	0.045*
negative regulation of viral genome replication	5	0.245	20.4	6.9×10^{-5}	0.051
regulation of immune response	8	1.097	7.289	7.9×10^{-5}	0.057
receptor activity	15	4.158	3.607	8.8×10^{-5}	0.064
peptidase activity	25	9.815	2.547	0.0001	0.074
receptor binding	21	7.473	2.810	0.0001	0.075

Continued on next page

Gene ontology	n_{Observed}	n_{Expected}	Odds ratio	p_v	p_v^{adj} (* if < 0.05)
membrane	185	122.7	1.508	0.00013	0.095
fibrinolysis	5	0.307	16.3	0.00013	0.096
negative regulation of blood coagulation	4	0.123	32.5	0.00016	0.115
neutrophil chemotaxis	6	0.612	9.797	0.00019	0.136
defense response to Gram-negative bacterium	6	0.612	9.797	0.00019	0.136
receptor-mediated endocytosis	11	2.549	4.315	0.0002	0.141
hydrolase activity	54	29.9	1.804	0.00021	0.151
acrosomal membrane	5	0.368	13.6	0.00023	0.166
response to virus	8	1.342	5.960	0.00024	0.172
antioxidant activity	4	0.185	21.7	0.00035	0.253
natural killer cell activation	4	0.185	21.7	0.00035	0.253
plasminogen activation	4	0.185	21.7	0.00035	0.253
positive regulation of angiogenesis	10	2.312	4.326	0.00037	0.264
positive regulation of phagocytosis	5	0.430	11.6	0.00038	0.269
negative regulation of endopeptidase activity	8	1.465	5.461	0.00039	0.277
blood coagulation	12	3.336	3.597	0.00043	0.308
organelle membrane	8	1.526	5.242	0.00049	0.346
cellular response to interleukin-1	6	0.797	7.532	0.00055	0.388
fatty acid metabolic process	11	3.039	3.620	0.0007	0.499
platelet alpha granule lumen	7	1.223	5.721	0.00071	0.505
defense response	6	0.858	6.993	0.00074	0.526
specific granule membrane	8	1.772	4.516	0.001	0.778
bile acid biosynthetic process	4	0.308	13.0	0.001	0.813
phospholipase A2 activity	4	0.308	13.0	0.001	0.813
cholesterol efflux	4	0.308	13.0	0.001	0.813
apoptotic cell clearance	4	0.308	13.0	0.001	0.813
arachidonic acid secretion	4	0.308	13.0	0.001	0.813

The genes detected under adaptation by mutation-selection codon models are enriched primarily with ontologies related to immune system processes (innate immune response, immune response, inflammatory response, defense response to virus, etc) and ontologies related to the external membrane (extracellular region, extracellular exosome, etc).

2.2 Site-specific ω -based model

For each gene, we computed the proportion of sites classified under an adaptive regime such that the lower bound for the posterior credibility interval of site-specific ω ($\alpha = 0.05$) is above 1. Because this is a unilateral test ($\omega > 1$) the risk is $\alpha/2 = 0.05/2 = 0.025$ for each site. For each ontology, the proportion of sites under adaptation is compared between the set of genes sharing this given ontology and the rest of the genes with Mann-Whitney U test. p_v^{adj} are corrected for multiple comparison (Holm-Bonferroni correction).

Table S2: Ontology enrichment with site-specific ω -based model

Gene ontology	Mann-Whitney U	p_v	p_v^{adj} (* if < 0.05)
extracellular region	2.1×10^6	1×10^{-17}	5.1×10^{-15}*
extracellular space	1.5×10^6	3.9×10^{-15}	2×10^{-12}*
immune system process	5.6×10^5	7.5×10^{-15}	3.7×10^{-12}*
immune response	3.7×10^5	2×10^{-12}	9.8×10^{-10}*
external side of plasma membrane	2.8×10^5	8.1×10^{-11}	4×10^{-8}*
innate immune response	4.8×10^5	6.9×10^{-10}	3.4×10^{-7}*
blood microparticle	1.6×10^5	2.6×10^{-9}	1.3×10^{-6}*
inflammatory response	4.1×10^5	2.1×10^{-8}	1×10^{-5}*
DNA repair	4.4×10^5	1.6×10^{-6}	0.0008*
lipid metabolic process	6.4×10^5	1.8×10^{-6}	0.00086*
serine-type endopeptidase activity	2.2×10^5	1.9×10^{-6}	0.0009*
receptor activity	3×10^5	3.3×10^{-6}	0.002*
cytokine activity	2.4×10^5	3.7×10^{-6}	0.002*
apical plasma membrane	4.1×10^5	4.7×10^{-6}	0.002*

Continued on next page

Gene ontology	Mann-Whitney U	p_v	p_v^{adj} (* if < 0.05)
cell surface receptor signaling pathway	3.4×10^5	5.9×10^{-6}	0.003*
integral component of plasma membrane	1.4×10^6	1.1×10^{-5}	0.005*
fatty acid metabolic process	2.2×10^5	1.1×10^{-5}	0.005*
cell surface	6.1×10^5	1.2×10^{-5}	0.006*
defense response to bacterium	1.5×10^5	1.5×10^{-5}	0.007*
centriole	1.7×10^5	1.5×10^{-5}	0.007*
leukocyte migration	2×10^5	1.5×10^{-5}	0.007*
proteolysis	7.2×10^5	2×10^{-5}	0.009*
cell-matrix adhesion	1.5×10^5	2×10^{-5}	0.009*
defense response to virus	1.7×10^5	2.1×10^{-5}	0.010*
cellular response to DNA damage stimulus	5.6×10^5	3.7×10^{-5}	0.017*
peroxisome	1.7×10^5	3.7×10^{-5}	0.018*
extracellular exosome	2.3×10^6	3.9×10^{-5}	0.018*
viral entry into host cell	1.2×10^5	6.1×10^{-5}	0.028*
lipid catabolic process	1.6×10^5	7.5×10^{-5}	0.035*
cellular protein metabolic process	2.3×10^5	9.6×10^{-5}	0.045*
integral component of membrane	3.8×10^6	0.00015	0.068
metallopeptidase activity	2.6×10^5	0.00017	0.081
serine-type peptidase activity	1.6×10^5	0.00019	0.088
platelet degranulation	1.7×10^5	0.00024	0.110
cilium	3.3×10^5	0.00026	0.118
peptidase activity	6.1×10^5	0.00026	0.121
neutrophil degranulation	5×10^5	0.00029	0.135
cell adhesion	6.2×10^5	0.00033	0.152
ciliary basal body-plasma membrane docking	1.4×10^5	0.00046	0.209
DNA replication	2×10^5	0.00053	0.243
meiotic cell cycle	1.7×10^5	0.00056	0.254
collagen trimer	1.3×10^5	0.00064	0.291
receptor-mediated endocytosis	1.9×10^5	0.00069	0.314
carbohydrate binding	1.9×10^5	0.0007	0.317
regulation of G2/M transition of mitotic cell cycle	1.2×10^5	0.001	0.516
steroid metabolic process	1.4×10^5	0.002	0.694
receptor binding	4.7×10^5	0.002	0.814
positive regulation of ERK1 and ERK2 cascade	2.3×10^5	0.002	0.884

The sites detected under adaptation by site-specific ω -based codon models are enriched primarily with ontologies related to immune system processes (innate immune response, immune response, inflammatory response, defense response to virus, etc) and ontologies related to the external membrane (extracellular region, extracellular exosome, etc).

2.3 Site-specific mutation-selection model

For each gene, we computed the proportion of sites classified under an adaptive regime such that the lower bound for the posterior credibility interval of site-specific ω ($\alpha = 0.05$) is above the upper bound of the posterior credibility interval of site-specific ω_0 ($\alpha = 0.05$). Because this is a unilateral test ($\omega > \omega_0$) and the two posterior credibility interval are independent, the risk is $(\alpha/2)^2 = 0.025^2 = 6.25 \times 10^{-4}$ for each site. For each ontology, the proportion of sites under adaptation is compared between the set of genes sharing this given ontology and the rest of the genes with Mann-Whitney U test. p_v^{adj} are corrected for multiple comparison (Holm-Bonferroni correction).

Table S3: Ontology enrichment with site-specific mutation-selection model

Gene ontology	Mann-Whitney U	p_v	p_v^{adj} (* if < 0.05)
extracellular space	1.6×10^6	8.4×10^{-22}	4.1×10^{-19}*
extracellular region	2.2×10^6	2.8×10^{-21}	1.4×10^{-18}*
lipid metabolic process	7.7×10^5	3.4×10^{-21}	1.7×10^{-18}*
oxidation-reduction process	8.8×10^5	1.6×10^{-19}	8×10^{-17}*
integral component of membrane	4.1×10^6	1.8×10^{-18}	8.6×10^{-16}*
oxidoreductase activity	7.8×10^5	3.2×10^{-17}	1.6×10^{-14}*

Continued on next page

Gene ontology	Mann-Whitney U	p_v	p_v^{adj} (* if < 0.05)
extracellular exosome	2.5×10^6	1.6×10^{-15}	7.8×10^{-13}*
immune system process	5.9×10^5	9.1×10^{-14}	4.5×10^{-11}*
immune response	4.1×10^5	2.1×10^{-13}	1×10^{-10}*
integral component of plasma membrane	1.5×10^6	5.4×10^{-13}	2.6×10^{-10}*
inflammatory response	4.6×10^5	3.3×10^{-12}	1.6×10^{-9}*
fatty acid metabolic process	2.7×10^5	1.3×10^{-11}	6.2×10^{-9}*
innate immune response	5.2×10^5	1.1×10^{-10}	5.3×10^{-8}*
mitochondrion	1.6×10^6	1.6×10^{-10}	7.5×10^{-8}*
serine-type endopeptidase activity	2.5×10^5	1.6×10^{-10}	7.8×10^{-8}*
metabolic process	5.9×10^5	1.7×10^{-10}	8.1×10^{-8}*
mitochondrial inner membrane	5×10^5	4.8×10^{-10}	2.3×10^{-7}*
blood microparticle	1.8×10^5	5×10^{-10}	2.4×10^{-7}*
external side of plasma membrane	2.9×10^5	4.3×10^{-9}	2.1×10^{-6}*
defense response to bacterium	1.8×10^5	3.9×10^{-8}	1.8×10^{-5}*
catalytic activity	6.5×10^5	7.5×10^{-8}	3.6×10^{-5}*
symporter activity	1.8×10^5	1.1×10^{-7}	5.4×10^{-5}*
membrane	4.7×10^6	1.2×10^{-7}	5.5×10^{-5}*
peroxisome	1.9×10^5	1.2×10^{-7}	5.6×10^{-5}*
cell surface	6.5×10^5	1.2×10^{-7}	5.7×10^{-5}*
apical plasma membrane	4.4×10^5	1.4×10^{-7}	6.6×10^{-5}*
serine-type peptidase activity	1.9×10^5	4.4×10^{-7}	0.00021*
hydrolase activity	1.7×10^6	5.7×10^{-7}	0.00027*
steroid metabolic process	1.7×10^5	6.6×10^{-7}	0.00031*
neutrophil degranulation	5.5×10^5	7.7×10^{-7}	0.00036*
flavin adenine dinucleotide binding	1.4×10^5	1×10^{-6}	0.00047*
proteolysis	7.6×10^5	2.1×10^{-6}	0.00096*
lipid catabolic process	1.7×10^5	2.2×10^{-6}	0.001*
plasma membrane	3.6×10^6	3.7×10^{-6}	0.002*
cellular protein metabolic process	2.5×10^5	5×10^{-6}	0.002*
lyase activity	2.2×10^5	5.6×10^{-6}	0.003*
lysosomal lumen	1.7×10^5	6.5×10^{-6}	0.003*
extracellular matrix disassembly	1.3×10^5	1.2×10^{-5}	0.005*
organelle membrane	1.4×10^5	1.3×10^{-5}	0.006*
peptidase activity	6.4×10^5	1.4×10^{-5}	0.006*
endoplasmic reticulum lumen	4.1×10^5	2×10^{-5}	0.009*
mitochondrial matrix	4.1×10^5	2.2×10^{-5}	0.010*
iron ion binding	1.9×10^5	2.3×10^{-5}	0.011*
sodium ion transport	2×10^5	2.9×10^{-5}	0.013*
response to lipopolysaccharide	2.3×10^5	3.4×10^{-5}	0.015*
cytokine activity	2.5×10^5	5.7×10^{-5}	0.026*
calcium ion binding	7.5×10^5	7.3×10^{-5}	0.033*
viral entry into host cell	1.3×10^5	7.7×10^{-5}	0.035*
receptor-mediated endocytosis	2×10^5	0.00011	0.049*
collagen catabolic process	1.3×10^5	0.00013	0.060
carbohydrate binding	2×10^5	0.00015	0.067
cholesterol metabolic process	1.5×10^5	0.00016	0.070
platelet degranulation	1.8×10^5	0.00017	0.075
defense response to virus	1.7×10^5	0.00017	0.075
specific granule membrane	1.5×10^5	0.00017	0.076
basolateral plasma membrane	2.5×10^5	0.00019	0.085
cell adhesion	6.4×10^5	0.00022	0.097
acrosomal vesicle	1.3×10^5	0.00023	0.101
cell-matrix adhesion	1.6×10^5	0.00024	0.104
leukocyte migration	2×10^5	0.00025	0.108
cell surface receptor signaling pathway	3.4×10^5	0.00025	0.109
collagen binding	1.3×10^5	0.00034	0.150
heme binding	1.4×10^5	0.00035	0.150
endoplasmic reticulum	1.5×10^6	0.00035	0.151
chemotaxis	1.7×10^5	0.00036	0.154
transmembrane transporter activity	1.6×10^5	0.00037	0.159
carbohydrate metabolic process	2.7×10^5	0.00037	0.159
transmembrane transport	6.6×10^5	0.00038	0.161
extracellular matrix organization	3×10^5	0.0006	0.256
centriole	1.6×10^5	0.001	0.440
adaptive immune response	1.7×10^5	0.001	0.462
cilium	3.4×10^5	0.001	0.493

Continued on next page

Gene ontology	Mann-Whitney U	p_v	p_v^{adj} (* if < 0.05)
receptor activity	2.9×10^5	0.001	0.542
collagen trimer	1.4×10^5	0.001	0.612
extracellular matrix	3.6×10^5	0.002	0.637
protease binding	1.4×10^5	0.002	0.637
intracellular membrane-bounded organelle	8.4×10^5	0.002	0.762
lipid transport	1.4×10^5	0.002	0.799

The sites detected under adaptation by mutation-selection codon models are enriched primarily with ontologies related to immune system processes (innate immune response, immune response, inflammatory response, defense response to virus, etc) and ontologies related to the external membrane (extracellular region, extracellular exosome, etc). The ontologies are similar to the sites detected by site-specific ω -based model, although with stronger statistical support (lower p_v^{adj}). Moreover, sites detected under adaptation by mutation-selection codon models are also enriched with ontologies related to oxidoreductase activities, oxidation-reduction process and mitochondrion, which are not found by site-specific ω -based model.

2.4 Exclusive to site-specific mutation-selection model

For each gene, we computed the proportion of sites classified under an adaptive regime such that the lower bound for the posterior credibility interval of site-specific ω ($\alpha = 0.05$) is above the upper bound of the posterior credibility interval of site-specific ω_0 ($\alpha = 0.05$), while the mean site-specific ω is below 1. Thus, these sites cannot be detected by site-specific mutation-selection model. Because this is a unilateral test ($\omega > \omega_0$) and the two posterior credibility interval are independent, the risk is $(\alpha/2)^2 = 0.025^2 = 6.25 \times 10^{-4}$ for each site. For each ontology, the proportion of sites under adaptation is compared between the set of genes sharing this given ontology and the rest of the genes with Mann-Whitney U test. p_v^{adj} are corrected for multiple comparison (Holm–Bonferroni correction).

Table S4: Ontology enrichment with sites exclusive to mutation-selection model

Gene ontology	Mann-Whitney U	p_v	p_v^{adj} (* if < 0.05)
oxidation-reduction process	9.1×10^5	9.3×10^{-26}	4.6×10^{-23}*
extracellular exosome	2.6×10^6	7.6×10^{-25}	3.8×10^{-22}*
oxidoreductase activity	8.1×10^5	7.5×10^{-24}	3.7×10^{-21}*
lipid metabolic process	7.7×10^5	1.6×10^{-21}	8.1×10^{-19}*
metabolic process	6.2×10^5	7×10^{-16}	3.4×10^{-13}*
transmembrane transport	7.5×10^5	1.1×10^{-14}	5.3×10^{-12}*
membrane	4.8×10^6	2.2×10^{-14}	1.1×10^{-11}*
plasma membrane	3.7×10^6	2.4×10^{-14}	1.2×10^{-11}*
integral component of membrane	4.1×10^6	1×10^{-13}	4.9×10^{-11}*
integral component of plasma membrane	1.5×10^6	6×10^{-13}	2.9×10^{-10}*
mitochondrion	1.7×10^6	9.6×10^{-13}	4.7×10^{-10}*
catalytic activity	6.9×10^5	1.1×10^{-12}	5.4×10^{-10}*
symporter activity	2×10^5	5.3×10^{-11}	2.5×10^{-8}*
ion transport	8×10^5	7.3×10^{-11}	3.5×10^{-8}*
transmembrane transporter activity	2×10^5	7.3×10^{-11}	3.5×10^{-8}*
endoplasmic reticulum	1.6×10^6	8×10^{-11}	3.8×10^{-8}*
fatty acid metabolic process	2.6×10^5	1.2×10^{-10}	5.7×10^{-8}*
mitochondrial inner membrane	4.9×10^5	5.6×10^{-10}	2.7×10^{-7}*
blood microparticle	1.7×10^5	2.3×10^{-9}	1.1×10^{-6}*
lysosomal lumen	1.8×10^5	5.9×10^{-9}	2.8×10^{-6}*
sodium ion transport	2.2×10^5	1.2×10^{-8}	5.7×10^{-6}*
apical plasma membrane	4.4×10^5	1×10^{-7}	4.8×10^{-5}*
flavin adenine dinucleotide binding	1.4×10^5	2×10^{-7}	9.4×10^{-5}*
basolateral plasma membrane	2.7×10^5	2.4×10^{-7}	0.00011*
calcium ion binding	7.7×10^5	2.4×10^{-7}	0.00011*
receptor-mediated endocytosis	2.1×10^5	3.5×10^{-7}	0.00016*
neutrophil degranulation	5.5×10^5	3.9×10^{-7}	0.00018*

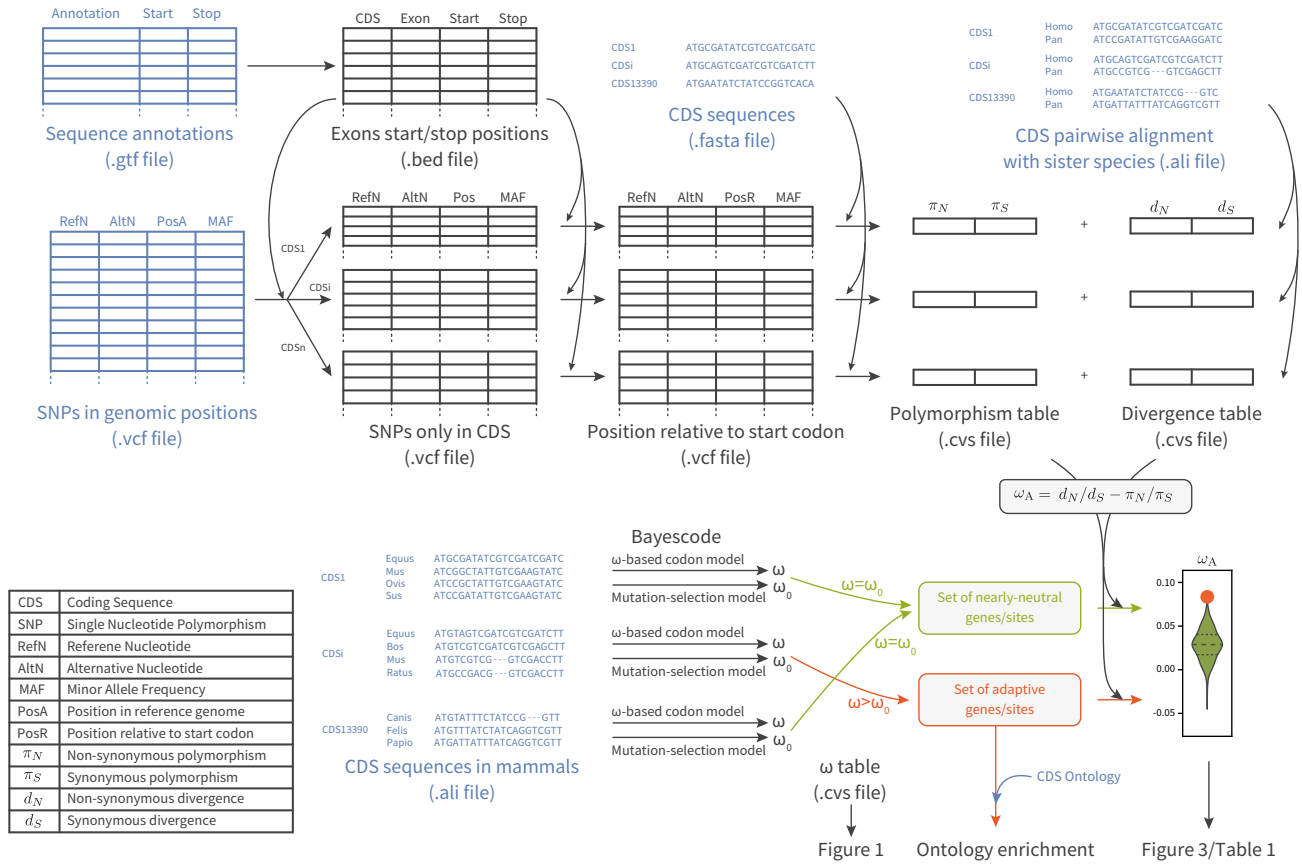
Continued on next page

Gene ontology	Mann-Whitney U	p_v	p_v^{adj} (* if < 0.05)
peroxisome	1.9×10^5	4.3×10^{-7}	0.0002*
iron ion binding	2×10^5	5.9×10^{-7}	0.00028*
steroid metabolic process	1.6×10^5	1.4×10^{-6}	0.00067*
hydrolase activity	1.7×10^6	2.8×10^{-6}	0.001*
endoplasmic reticulum lumen	4.1×10^5	2.8×10^{-6}	0.001*
endoplasmic reticulum membrane	1×10^6	4.2×10^{-6}	0.002*
mitochondrial matrix	4.2×10^5	6.9×10^{-6}	0.003*
ligase activity	2.2×10^5	8.1×10^{-6}	0.004*
lyase activity	2.1×10^5	8.3×10^{-6}	0.004*
cellular protein metabolic process	2.5×10^5	1.1×10^{-5}	0.005*
intracellular membrane-bounded organelle	8.7×10^5	1.4×10^{-5}	0.006*
extracellular space	1.4×10^6	1.5×10^{-5}	0.007*
external side of plasma membrane	2.6×10^5	2.2×10^{-5}	0.010*
lipid transport	1.5×10^5	3.2×10^{-5}	0.015*
heme binding	1.5×10^5	3.6×10^{-5}	0.016*
organelle membrane	1.3×10^5	5×10^{-5}	0.023*
serine-type endopeptidase activity	2.2×10^5	9.8×10^{-5}	0.045*
endosome membrane	2.9×10^5	0.00013	0.060
extracellular matrix organization	3.1×10^5	0.00013	0.060
serine-type peptidase activity	1.7×10^5	0.00017	0.075
transporter activity	1.9×10^5	0.00019	0.084
lysosome	4.8×10^5	0.00022	0.097
phospholipid binding	1.5×10^5	0.00031	0.136
ATP binding	1.6×10^6	0.00034	0.151
peptidase activity	6.2×10^5	0.00038	0.168
carbohydrate metabolic process	2.6×10^5	0.00041	0.184
structural molecule activity	2.1×10^5	0.00045	0.198
myelin sheath	1.7×10^5	0.00052	0.229
platelet degranulation	1.7×10^5	0.00058	0.256
cholesterol metabolic process	1.4×10^5	0.00062	0.272
isomerase activity	1.2×10^5	0.00067	0.292
specific granule membrane	1.4×10^5	0.00088	0.386
chemotaxis	1.7×10^5	0.00095	0.413
proteolysis	7.2×10^5	0.001	0.436
sarcolemma	1.4×10^5	0.001	0.470
extracellular matrix	3.6×10^5	0.001	0.543
transferase activity	1.8×10^6	0.001	0.563
membrane raft	2.8×10^5	0.002	0.676
actin filament binding	1.7×10^5	0.002	0.677
cell surface	6×10^5	0.002	0.697
collagen catabolic process	1.2×10^5	0.002	0.703
calcium ion transmembrane transport	1.5×10^5	0.002	0.727
regulation of ion transmembrane transport	1.8×10^5	0.002	0.915
calcium ion transport	1.6×10^5	0.002	0.981

The sites detected under adaptation solely by mutation-selection codon models (with $\omega < 1$) are enriched primarily with ontologies related to oxidoreductase activities, oxidation-reduction and mitochondrion process as well as ontologies related to the membrane (transmembrane transport, integral component of membrane, transmembrane transporter activity, etc).

3 Graphical abstract for the pipeline.

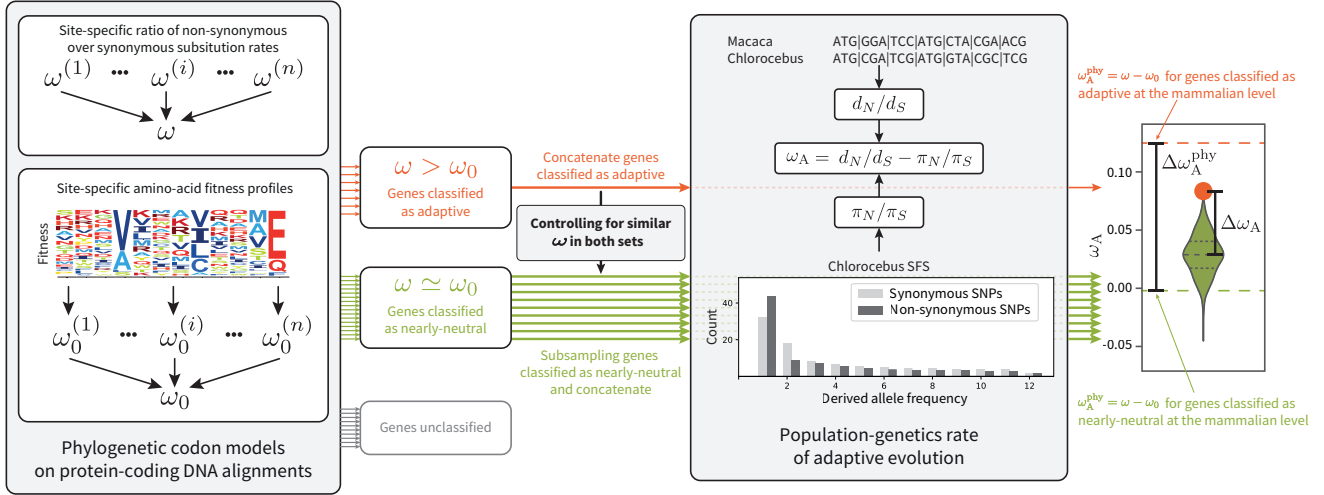
Figure S2:



4 Rate of adaptation enrichment while controlling for ω

ω is controlled to be the same in the nearly-neutral replicate and the adaptive set of genes, such as to alleviate the fact that genes classified as adaptive have a higher ω than genes classified as nearly-neutral, which could bias our comparison since ω_A could simply be higher for genes with higher ω .

Figure S3:



The random sampling is weighted to control for ω in the set of nearly-neutral genes/sites. First, a normal distribution is fitted to ω in both sets, and the probability density is called f for the adaptive set and g for the nearly-neutral set. Secondly, for each gene/site classified as nearly-neutral the weight is computed as the ratio $f(\omega)/g(\omega)$ for this specific gene/site. Sampling with this procedure produce a set of genes/sites classified as nearly-neutral with the same ω on average than the set of adaptive genes/sites.

4.1 Mutation-selection codon model at gene level ($\alpha = 0.05$)

Figure S4:

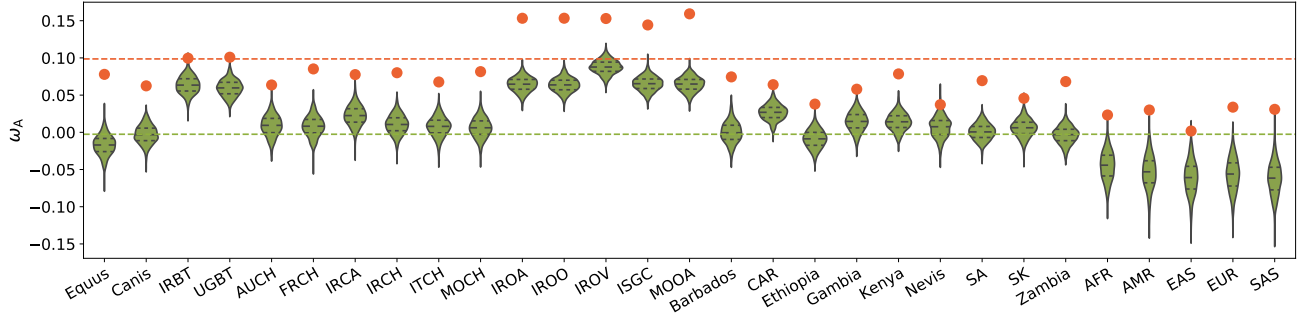


Table S5:

Population	Species	ω_A Adaptive	$\langle \omega_A \rangle$ Nearly-neutral	$\Delta\omega_A$	p_v	p_v^{adj}	$\frac{\Delta\omega_A}{\omega_A^{\text{phy}}}$	π_S
Diverse (Equus)	Equus caballus	0.078	-0.017	0.095	0.0	0.0*	0.952	0.002
Diverse (Canis)	Canis familiaris	0.062	-0.003	0.065	0.0	0.0*	0.639	0.004
Iran (IRBT)	Bos taurus	0.100	0.064	0.036	0.002	0.006*	0.356	0.007
Uganda (UGBT)	Bos taurus	0.101	0.059	0.041	0.0	0.0*	0.412	0.008
Australia (AUCH)	Capra hircus	0.064	0.009	0.055	0.0	0.0*	0.541	0.003
France (FRCH)	Capra hircus	0.085	0.008	0.077	0.0	0.0*	0.764	0.002
Iran (IRCA)	Capra aegagrus	0.078	0.022	0.055	0.0	0.0*	0.544	0.003
Iran (IRCH)	Capra hircus	0.080	0.011	0.070	0.0	0.0*	0.688	0.004
Italy (ITCH)	Capra hircus	0.068	0.008	0.060	0.0	0.0*	0.594	0.003
Morocco (MOCH)	Capra hircus	0.082	0.006	0.076	0.0	0.0*	0.748	0.004
Iran (IROA)	Ovis aries	0.153	0.064	0.089	0.0	0.0*	0.878	0.007
Iran (IROO)	Ovis orientalis	0.153	0.064	0.090	0.0	0.0*	0.886	0.008
Iran (IROV)	Ovis vignei	0.153	0.088	0.065	0.0	0.0*	0.642	0.005
Various (ISGC)	Ovis aries	0.144	0.065	0.079	0.0	0.0*	0.780	0.008
Morocco (MOOA)	Ovis aries	0.159	0.065	0.095	0.0	0.0*	0.934	0.007
Barbados	Chlorocebus sabaeus	0.074	-0.0002	0.075	0.0	0.0*	0.737	0.003
Central African Republic (CAR)	Chlorocebus sabaeus	0.064	0.027	0.037	0.0	0.0*	0.368	0.006
Ethiopia	Chlorocebus sabaeus	0.038	-0.009	0.047	0.0	0.0*	0.461	0.005
Gambia	Chlorocebus sabaeus	0.058	0.014	0.043	0.0	0.0*	0.429	0.005
Kenya	Chlorocebus sabaeus	0.079	0.014	0.064	0.0	0.0*	0.634	0.004
Nevis	Chlorocebus sabaeus	0.037	0.007	0.030	0.020	0.020*	0.300	0.003
South Africa (SA)	Chlorocebus sabaeus	0.069	0.00053	0.069	0.0	0.0*	0.680	0.006
Saint Kitts (SK)	Chlorocebus sabaeus	0.046	0.006	0.040	0.001	0.004*	0.393	0.004
Zambia	Chlorocebus sabaeus	0.068	-0.004	0.072	0.0	0.0*	0.709	0.006
African (AFR)	Homo sapiens	0.023	-0.045	0.068	0.0	0.0*	0.672	0.002
Ad Mixed American (AMR)	Homo sapiens	0.030	-0.054	0.083	0.0	0.0*	0.825	0.002
East Asian (EAS)	Homo sapiens	0.002	-0.061	0.063	0.002	0.006*	0.620	0.002
European (EUR)	Homo sapiens	0.034	-0.057	0.091	0.0	0.0*	0.896	0.002
South Asian (SAS)	Homo sapiens	0.031	-0.062	0.093	0.0	0.0*	0.917	0.002

Figure S5:

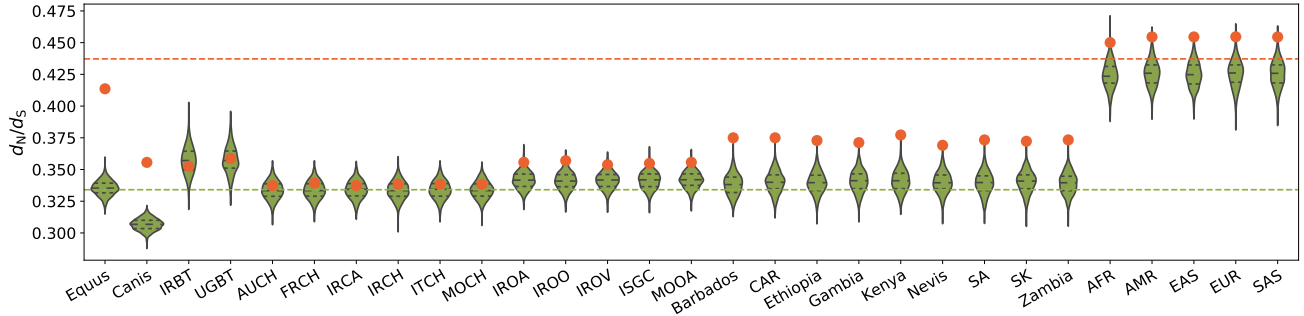


Table S6:

Population	Species	d_N/d_S	$\langle d_N/d_S \rangle$	p_v	p_v^{adj}	π_S
		Adaptive	Nearly-neutral			
Diverse (Equus)	Equus caballus	0.414	0.335	0.0	0.0*	0.002
Diverse (Canis)	Canis familiaris	0.356	0.307	0.0	0.0*	0.004
Iran (IRBT)	Bos taurus	0.352	0.357	0.657	1.000	0.007
Uganda (UGBT)	Bos taurus	0.359	0.358	0.432	1.000	0.008
Australia (AUCH)	Capra hircus	0.337	0.334	0.312	1.000	0.003
France (FRCH)	Capra hircus	0.339	0.334	0.223	1.000	0.002
Iran (IRCA)	Capra aegagrus	0.337	0.334	0.338	1.000	0.003
Iran (IRCH)	Capra hircus	0.338	0.334	0.257	1.000	0.004
Italy (ITCH)	Capra hircus	0.338	0.334	0.278	1.000	0.003
Morocco (MOCH)	Capra hircus	0.338	0.334	0.252	1.000	0.004
Iran (IROA)	Ovis aries	0.356	0.342	0.021	0.231	0.007
Iran (IROO)	Ovis orientalis	0.357	0.341	0.013	0.169	0.008
Iran (IROV)	Ovis vignei	0.354	0.342	0.037	0.333	0.005
Various (ISGC)	Ovis aries	0.355	0.342	0.025	0.250	0.008
Morocco (MOOA)	Ovis aries	0.356	0.342	0.017	0.204	0.007
Barbados	Chlorocebus sabaesus	0.375	0.338	0.0	0.0*	0.003
Central African Republic (CAR)	Chlorocebus sabaesus	0.375	0.340	0.0	0.0*	0.006
Ethiopia	Chlorocebus sabaesus	0.373	0.340	0.0	0.0*	0.005
Gambia	Chlorocebus sabaesus	0.371	0.341	0.0	0.0*	0.005
Kenya	Chlorocebus sabaesus	0.377	0.341	0.0	0.0*	0.004
Nevis	Chlorocebus sabaesus	0.369	0.340	0.0	0.0*	0.003
South Africa (SA)	Chlorocebus sabaesus	0.373	0.339	0.0	0.0*	0.006
Saint Kitts (SK)	Chlorocebus sabaesus	0.372	0.340	0.0	0.0*	0.004
Zambia	Chlorocebus sabaesus	0.373	0.339	0.0	0.0*	0.006
African (AFR)	Homo sapiens	0.450	0.424	0.005	0.075	0.002
Ad Mixed American (AMR)	Homo sapiens	0.455	0.426	0.002	0.034*	0.002
East Asian (EAS)	Homo sapiens	0.454	0.425	0.0	0.0*	0.002
European (EUR)	Homo sapiens	0.455	0.426	0.003	0.048*	0.002
South Asian (SAS)	Homo sapiens	0.454	0.425	0.005	0.075	0.002

In *Bos*, *Capras* and *Ovis*, d_N/d_S computed for the set of genes under adaptation at the phylogenetic scale (red, $1 > \omega > \omega_0$) is not higher than for the set of genes under a nearly-neutral regime (green, $1 > \omega \simeq \omega_0$), showing that the sampling procedure controlling for ω at the phylogenetic scale is valid. However, even though d_N/d_S is not higher (genes are not faster overall), the rate of adaptation at the population-genetic scale (ω_A) for the set of genes supposedly under adaptation is higher than for the set of nearly-neutral genes in all populations. Altogether, these genes have a higher rate of adaptation, while not evolving faster than their nearly-neutral counterpart, showing that the rate of adaptation computed at the phylogenetic scale is able to detect genes under pervasive adaptation.

4.2 Mutation-selection codon model at site level ($\alpha = 0.05$)

Figure S6:

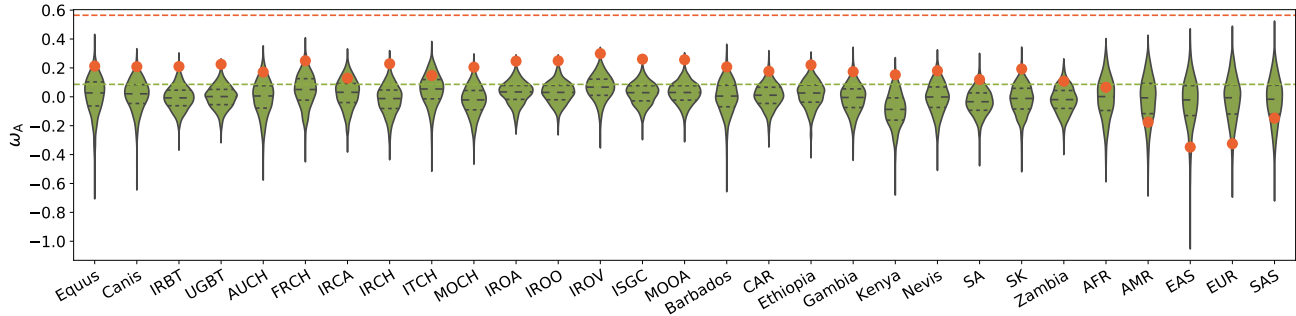


Table S7:

Population	Species	ω_A Adaptive	$\langle \omega_A \rangle$ Nearly-neutral	$\Delta\omega_A$	p_V	p_V^{adj}	$\frac{\Delta\omega_A}{\omega_A^{\text{phy}}}$	π_S
Diverse (Equus)	Equus caballus	0.213	0.010	0.203	0.034	0.374	0.425	0.002
Diverse (Canis)	Canis familiaris	0.208	0.013	0.195	0.013	0.234	0.407	0.004
Iran (IRBT)	Bos taurus	0.210	-0.007	0.217	0.005	0.110	0.454	0.007
Uganda (UGBT)	Bos taurus	0.225	-0.002	0.227	0.0	0.0*	0.476	0.008
Australia (AUCH)	Capra hircus	0.171	-0.006	0.177	0.056	0.504	0.369	0.003
France (FRCH)	Capra hircus	0.249	0.046	0.204	0.025	0.336	0.425	0.002
Iran (IRCA)	Capra aegagrus	0.129	0.023	0.106	0.149	1.000	0.221	0.003
Iran (IRCH)	Capra hircus	0.229	-0.020	0.249	0.004	0.092	0.519	0.004
Italy (ITCH)	Capra hircus	0.148	0.048	0.099	0.170	1.000	0.207	0.003
Morocco (MOCH)	Capra hircus	0.205	-0.026	0.231	0.009	0.171	0.482	0.004
Iran (IROA)	Ovis aries	0.247	0.028	0.219	0.002	0.048*	0.456	0.007
Iran (IROO)	Ovis orientalis	0.249	0.029	0.220	0.001	0.026*	0.458	0.008
Iran (IROV)	Ovis vignei	0.299	0.063	0.236	0.0	0.0*	0.493	0.005
Various (ISGC)	Ovis aries	0.261	0.024	0.237	0.0	0.0*	0.493	0.008
Morocco (MOOA)	Ovis aries	0.257	0.026	0.231	0.001	0.026*	0.481	0.007
Barbados	Chlorocebus sabaeus	0.207	0.00044	0.206	0.017	0.272	0.432	0.003
Central African Republic (CAR)	Chlorocebus sabaeus	0.177	0.008	0.168	0.017	0.272	0.353	0.006
Ethiopia	Chlorocebus sabaeus	0.220	0.018	0.202	0.008	0.160	0.423	0.005
Gambia	Chlorocebus sabaeus	0.174	-0.011	0.185	0.024	0.336	0.387	0.005
Kenya	Chlorocebus sabaeus	0.152	-0.088	0.240	0.006	0.126	0.503	0.004
Nevis	Chlorocebus sabaeus	0.180	-0.008	0.189	0.031	0.372	0.395	0.003
South Africa (SA)	Chlorocebus sabaeus	0.120	-0.036	0.155	0.034	0.374	0.325	0.006
Saint Kitts (SK)	Chlorocebus sabaeus	0.193	-0.018	0.211	0.013	0.234	0.441	0.004
Zambia	Chlorocebus sabaeus	0.108	-0.021	0.129	0.067	0.536	0.269	0.006
African (AFR)	Homo sapiens	0.066	-0.009	0.075	0.325	1.000	0.157	0.002
Ad Mixed American (AMR)	Homo sapiens	-0.175	-0.019	-0.157	0.849	1.000	-0.328	0.002
East Asian (EAS)	Homo sapiens	-0.348	-0.036	-0.312	0.953	1.000	-0.653	0.002
European (EUR)	Homo sapiens	-0.325	-0.021	-0.304	0.965	1.000	-0.636	0.002
South Asian (SAS)	Homo sapiens	-0.148	-0.025	-0.122	0.798	1.000	-0.256	0.002

Figure S7:

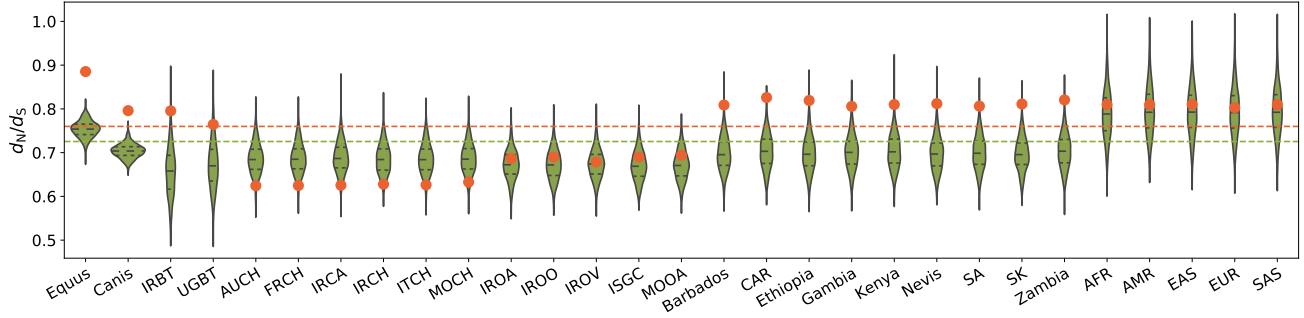


Table S8:

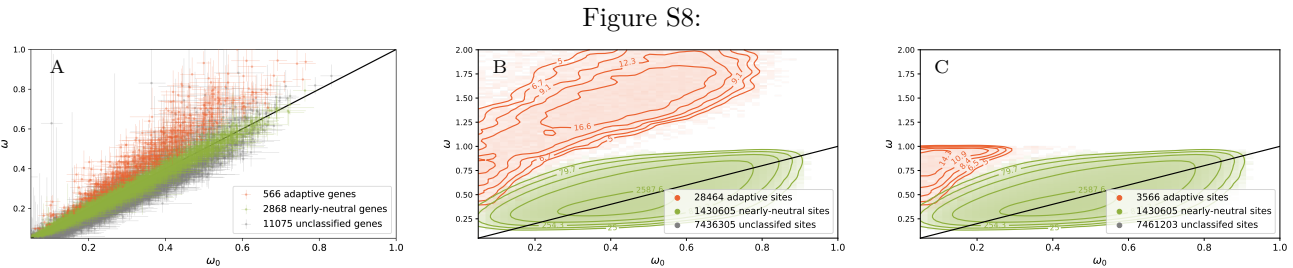
Population	Species	d_N/d_S Adaptive	$\langle d_N/d_S \rangle$ Nearly-neutral	p_v	p_v^{adj}	π_S
Diverse (Equus)	Equus caballus	0.885	0.754	0.0	0.0*	0.002
Diverse (Canis)	Canis familiaris	0.796	0.704	0.0	0.0*	0.004
Iran (IRBT)	Bos taurus	0.796	0.658	0.008	0.152	0.007
Uganda (UGBT)	Bos taurus	0.765	0.672	0.046	0.782	0.008
Australia (AUCH)	Capra hircus	0.624	0.686	0.972	1.000	0.003
France (FRCH)	Capra hircus	0.625	0.687	0.977	1.000	0.002
Iran (IRCA)	Capra aegagrus	0.626	0.690	0.977	1.000	0.003
Iran (IRCH)	Capra hircus	0.628	0.685	0.968	1.000	0.004
Italy (ITCH)	Capra hircus	0.626	0.686	0.970	1.000	0.003
Morocco (MOCH)	Capra hircus	0.633	0.686	0.948	1.000	0.004
Iran (IROA)	Ovis aries	0.687	0.672	0.331	1.000	0.007
Iran (IROO)	Ovis orientalis	0.690	0.672	0.298	1.000	0.008
Iran (IROV)	Ovis vignei	0.679	0.674	0.431	1.000	0.005
Various (ISGC)	Ovis aries	0.690	0.670	0.273	1.000	0.008
Morocco (MOOA)	Ovis aries	0.694	0.671	0.245	1.000	0.007
Barbados	Chlorocebus sabaesus	0.809	0.698	0.005	0.115	0.003
Central African Republic (CAR)	Chlorocebus sabaesus	0.826	0.704	0.003	0.081	0.006
Ethiopia	Chlorocebus sabaesus	0.819	0.697	0.003	0.081	0.005
Gambia	Chlorocebus sabaesus	0.806	0.702	0.012	0.216	0.005
Kenya	Chlorocebus sabaesus	0.810	0.703	0.006	0.126	0.004
Nevis	Chlorocebus sabaesus	0.812	0.697	0.004	0.100	0.003
South Africa (SA)	Chlorocebus sabaesus	0.806	0.701	0.007	0.140	0.006
Saint Kitts (SK)	Chlorocebus sabaesus	0.811	0.697	0.004	0.100	0.004
Zambia	Chlorocebus sabaesus	0.821	0.704	0.005	0.115	0.006
African (AFR)	Homo sapiens	0.810	0.790	0.351	1.000	0.002
Ad Mixed American (AMR)	Homo sapiens	0.810	0.796	0.378	1.000	0.002
East Asian (EAS)	Homo sapiens	0.810	0.794	0.382	1.000	0.002
European (EUR)	Homo sapiens	0.803	0.794	0.432	1.000	0.002
South Asian (SAS)	Homo sapiens	0.810	0.795	0.383	1.000	0.002

In *Bos*, *Capras*, *Ovis*, *Chlorocebus* and *Homo*, d_N/d_S computed for the set of sites under adaptation (red, $1 > \omega > \omega_0$) at the phylogenetic scale is not higher than for the set of sites under a nearly-neutral regime (green, $1 > \omega \simeq \omega_0$), showing that the sampling procedure controlling for ω at the phylogenetic scale is valid. However, even though d_N/d_S is not higher (sites are not faster overall), the rate of adaptation at the population-genetic scale (ω_A) for the set of sites supposedly under adaptation is higher than for the set of nearly-neutral sites in *Bos* and *Ovis*. Altogether, these sites have a higher rate of adaptation, while not evolving faster than their nearly-neutral counterpart, showing that the rate of adaptation computed at the phylogenetic scale is able to detect sites under pervasive adaptation, even though these sites are with $\omega < 1$ and thus cannot be detected by site-specific ω -based codon models.

5 Rate of adaptation enrichment with $\alpha = 0.005$

For each protein-coding DNA alignment, the Monte-Carlo Markov-Chain (MCMC) is run during 2000 points using the [BayesCode](#) software, after a burn-in of 1000 points. The mean of ω and ω_0 are computed across the MCMC (after burn-in), as well as the 99.5% posterior credibility interval ($\alpha = 0.005$) for each gene and site, which is more stringent than the 95% interval ($\alpha = 0.05$) as shown in the main manuscript. Genes and sites classified under an adaptive regime (in red) are rejecting the nearly-neutral assumption such that a lower bound for the posterior credibility interval of ω is above the upper bound of the posterior credibility interval of ω_0 , meaning $\omega > \omega_0$. Genes and sites are classified under a nearly-neutral regime (in green) if the average ω is within the posterior credibility interval of the ω_0 , and respectively the average ω_0 is also within the posterior credibility interval of ω , meaning $\omega = \omega_0$. Genes and sites that do not fall in any of these categories are considered unclassified.

5.1 Scatterplot with $\alpha = 0.005$



ω estimated by the site model against ω_0 calculated by the mutation-selection model. Scatter plot of 14,509 genes in panel A, with 99.5% posterior credibility interval ($\alpha = 0.005$). Density plot of sites in panel B and C. Genes or sites are then classified whether they detected as adaptive ($\omega > \omega_0$ in red) or nearly-neutral ($\omega \simeq \omega_0$ in green). In panel C, the set of sites detected exclusively by mutation-selection codon models have a mean $\omega < 1$.

5.2 Mutation-selection codon model at gene level ($\alpha = 0.005$)

Figure S9:

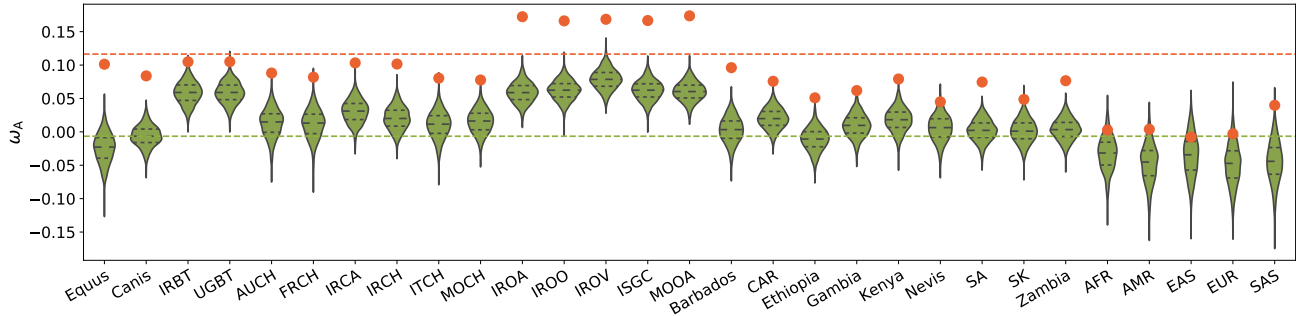


Table S9:

Population	Species	ω_A Adaptive	$\langle \omega_A \rangle$ Nearly-neutral	$\Delta\omega_A$	p_v	p_v^{adj}	$\frac{\Delta\omega_A}{\omega^{\text{phy}}_A}$	π_S
Diverse (Equus)	Equus caballus	0.101	-0.024	0.125	0.0	0.0*	1.029	0.002
Diverse (Canis)	Canis familiaris	0.084	-0.006	0.090	0.0	0.0*	0.722	0.004
Iran (IRBT)	Bos taurus	0.105	0.058	0.046	0.002	0.014*	0.381	0.008
Uganda (UGBT)	Bos taurus	0.105	0.059	0.046	0.001	0.010*	0.382	0.008
Australia (AUCH)	Capra hircus	0.088	0.013	0.075	0.0	0.0*	0.611	0.003
France (FRCH)	Capra hircus	0.082	0.012	0.070	0.001	0.010*	0.573	0.003
Iran (IRCA)	Capra aegagrus	0.103	0.031	0.073	0.0	0.0*	0.593	0.004
Iran (IRCH)	Capra hircus	0.102	0.020	0.081	0.0	0.0*	0.662	0.004
Italy (ITCH)	Capra hircus	0.080	0.010	0.070	0.0	0.0*	0.571	0.003
Morocco (MOCH)	Capra hircus	0.078	0.016	0.062	0.0	0.0*	0.504	0.004
Iran (IROA)	Ovis aries	0.172	0.059	0.113	0.0	0.0*	0.919	0.007
Iran (IROO)	Ovis orientalis	0.166	0.062	0.104	0.0	0.0*	0.841	0.009
Iran (IROV)	Ovis vignei	0.169	0.079	0.090	0.0	0.0*	0.726	0.005
Various (ISGC)	Ovis aries	0.167	0.062	0.105	0.0	0.0*	0.847	0.008
Morocco (MOOA)	Ovis aries	0.174	0.060	0.113	0.0	0.0*	0.916	0.008
Barbados	Chlorocebus sabaeus	0.096	0.003	0.093	0.0	0.0*	0.755	0.003
Central African Republic (CAR)	Chlorocebus sabaeus	0.076	0.020	0.056	0.0	0.0*	0.451	0.006
Ethiopia	Chlorocebus sabaeus	0.051	-0.011	0.062	0.0	0.0*	0.504	0.005
Gambia	Chlorocebus sabaeus	0.062	0.010	0.052	0.0	0.0*	0.423	0.005
Kenya	Chlorocebus sabaeus	0.079	0.018	0.061	0.0	0.0*	0.497	0.004
Nevis	Chlorocebus sabaeus	0.045	0.006	0.039	0.014	0.070	0.319	0.003
South Africa (SA)	Chlorocebus sabaeus	0.075	0.002	0.072	0.0	0.0*	0.587	0.006
Saint Kitts (SK)	Chlorocebus sabaeus	0.049	0.001	0.047	0.002	0.014*	0.384	0.004
Zambia	Chlorocebus sabaeus	0.077	0.004	0.073	0.0	0.0*	0.589	0.006
African (AFR)	Homo sapiens	0.003	-0.033	0.036	0.071	0.174	0.289	0.002
Ad Mixed American (AMR)	Homo sapiens	0.004	-0.047	0.051	0.033	0.132	0.415	0.002
East Asian (EAS)	Homo sapiens	-0.008	-0.036	0.028	0.186	0.186	0.227	0.002
European (EUR)	Homo sapiens	-0.003	-0.049	0.046	0.058	0.174	0.376	0.002
South Asian (SAS)	Homo sapiens	0.040	-0.045	0.084	0.001	0.010*	0.688	0.002

5.3 Mutation-selection codon model at site level ($\alpha = 0.005$)

Figure S10:

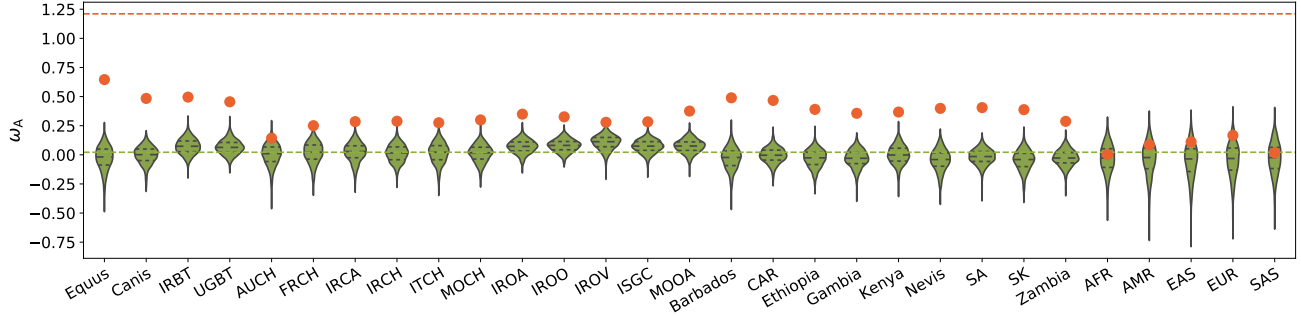


Table S10:

Population	Species	ω_A Adaptive	$\langle \omega_A \rangle$ Nearly-neutral	$\Delta\omega_A$	p_v	p_v^{adj}	$\frac{\Delta\omega_A}{\omega_A^{\text{phy}}}$	π_S
Diverse (Equus)	Equus caballus	0.646	-0.028	0.674	0.0	0.0*	0.567	0.002
Diverse (Canis)	Canis familiaris	0.484	-0.003	0.487	0.0	0.0*	0.406	0.004
Iran (IRBT)	Bos taurus	0.495	0.072	0.423	0.0	0.0*	0.356	0.008
Uganda (UGBT)	Bos taurus	0.455	0.065	0.390	0.0	0.0*	0.328	0.008
Australia (AUCH)	Capra hircus	0.143	0.001	0.142	0.043	0.258	0.119	0.003
France (FRCH)	Capra hircus	0.250	0.017	0.233	0.0	0.0*	0.196	0.003
Iran (IRCA)	Capra aegagrus	0.285	0.021	0.264	0.0	0.0*	0.222	0.004
Iran (IRCH)	Capra hircus	0.288	0.012	0.276	0.0	0.0*	0.233	0.004
Italy (ITCH)	Capra hircus	0.275	0.015	0.260	0.0	0.0*	0.219	0.003
Morocco (MOCH)	Capra hircus	0.299	0.012	0.287	0.0	0.0*	0.242	0.004
Iran (IROA)	Ovis aries	0.349	0.070	0.279	0.0	0.0*	0.235	0.007
Iran (IROO)	Ovis orientalis	0.326	0.078	0.248	0.0	0.0*	0.209	0.009
Iran (IROV)	Ovis vignei	0.279	0.106	0.174	0.0	0.0*	0.146	0.005
Various (ISGC)	Ovis aries	0.284	0.072	0.211	0.0	0.0*	0.178	0.008
Morocco (MOOA)	Ovis aries	0.376	0.074	0.302	0.0	0.0*	0.254	0.008
Barbados	Chlorocebus sabaeus	0.490	-0.031	0.521	0.0	0.0*	0.438	0.003
Central African Republic (CAR)	Chlorocebus sabaeus	0.467	-0.006	0.473	0.0	0.0*	0.398	0.006
Ethiopia	Chlorocebus sabaeus	0.390	-0.032	0.422	0.0	0.0*	0.355	0.005
Gambia	Chlorocebus sabaeus	0.356	-0.031	0.388	0.0	0.0*	0.326	0.005
Kenya	Chlorocebus sabaeus	0.367	-0.00077	0.368	0.0	0.0*	0.310	0.004
Nevis	Chlorocebus sabaeus	0.399	-0.045	0.444	0.0	0.0*	0.373	0.003
South Africa (SA)	Chlorocebus sabaeus	0.405	-0.017	0.422	0.0	0.0*	0.355	0.006
Saint Kitts (SK)	Chlorocebus sabaeus	0.388	-0.048	0.436	0.0	0.0*	0.366	0.004
Zambia	Chlorocebus sabaeus	0.288	-0.028	0.315	0.0	0.0*	0.265	0.006
African (AFR)	Homo sapiens	0.002	-0.034	0.036	0.423	0.794	0.030	0.002
Ad Mixed American (AMR)	Homo sapiens	0.086	-0.041	0.127	0.170	0.510	0.107	0.002
East Asian (EAS)	Homo sapiens	0.111	-0.052	0.164	0.107	0.428	0.138	0.002
European (EUR)	Homo sapiens	0.167	-0.045	0.212	0.059	0.295	0.178	0.002
South Asian (SAS)	Homo sapiens	0.017	-0.031	0.048	0.397	0.794	0.040	0.002

With a threshold of $\alpha = 0.005$ more stringent than as shown in the main manuscript ($\alpha = 0.05$), the rate of false positive is mechanically lower both at the site and gene level. However, the statistical power to test for enrichment of adaptation is not necessarily higher since we are working with fewer data. We thus obtain high values of ω_A for the set of genes and sites supposedly under adaptation at the phylogenetic scale, which also leads to higher $\Delta\omega_A$ when compared to the set of genes and sites supposedly under a nearly-neutral regime. Since we have more variance due to less data (violin plots are more extended for the set of nearly-neutral replicates), this higher value of the statistic $\Delta\omega_A$ does not translate to lower p_v^{adj} . We thus have to find a compromise between having large enough dataset to perform reliable computation of ω_A and having a very low rate of false positive for sites and genes under adaptation at the phylogenetic scale. Hence in the manuscript we settled with a rate of $\simeq 1\%$ FDR at the gene level and $\simeq 5\%$ FDR at the site level.

6 Rate of adaptation enrichment with polyDFE

The probability to sample allele at a given frequency (before fixation or extinction) is informative of its scaled selection coefficient at the population scale (β). Pooled across many sites, the SFS is thus informative on the underlying β of mutations, given we have a neutral expectation. In this configuration, a single β for all sampled mutations is biologically not realistic. Accordingly, a distribution of fitness effects of mutations (DFE) is assumed, usually modeled as a continuous distribution[1, 2]. In this study, we used the software polyDFE[3, 4] with model C (continuous distribution) and D (discrete distribution).

PolyDFE requires one SFS for non-synonymous mutations and one for synonymous mutations (neutral expectation), as well as the total number of sites on which each SFS has been sampled. From the SFS and the number of sites for both synonymous and non-synonymous changes, polyDFE estimates parameters of the DFE ($\phi(\beta)$) using maximum likelihood. The estimated DFE allows to subsequently computed the rate of adaptive evolution $\omega_A^{\text{polyDFE}}$.

polyDFE Model C

In model C, the DFE (ϕ) is given by a mixture of a Γ and Exponential distributions, parameterized by β_d , b , p_b and β_b as:

$$\phi(\beta) = \begin{cases} (1 - p_b) f_{\Gamma}(-\beta; -\beta_d, b) & \text{if } \beta \leq 0, \\ p_b f_e(\beta; \beta_b) & \text{if } \beta > 0, \end{cases} \quad (3)$$

where $\beta_d < 0$ is the estimated mean of the DFE for $\beta \leq 0$, $b > 0$ is the shape of the Γ distribution fixed to 1.0, $0 \leq p_b \leq 1$ is the estimated probability that $\beta > 0$, $\beta_b > 0$ is the mean of the DFE for $\beta > 0$ fixed to 4.0, and $f_{\Gamma}(x; m, b)$ is the density of the Γ distribution with mean m and shape b , while $f_e(x; m)$ is the density of the Exponential distribution with mean m .

polyDFE Model D

In model D, the DFE (ϕ) is given as a discrete distribution, where the selection coefficients can take one of β_i distinct values, $1 \leq i \leq K$, where each value β_i has probability p_i , with

$$\sum_{i=0}^K p_i = 1. \quad (4)$$

6.1 PolyDFE model C - including divergence data

The rate of adaptation $\omega_A^{\text{polyDFE}}$ is computed as the difference between the total rate of evolution $\omega = d_N/d_S$ obtained from divergence data and the rate of non-adaptive evolution ($\omega_{\text{NA}}(\phi)$) obtained from polymorphism data as in Tataru *et al.* [3]:

$$\omega_A^{\text{polyDFE}} = \omega - \omega_{\text{NA}}(\phi), \quad (5)$$

$$= d_N/d_S - \omega_{\text{NA}}(\phi). \quad (6)$$

Formally, $\omega_{\text{NA}}(\phi)$ is computed as the average fixation probability of mutations ($\mathbb{P}_{\text{fix}}(\beta)$) over the probability distribution given by the DFE $\phi(\beta)$, taken only for the negatively selected mutations ($\beta < 0$) as:

$$\omega_{\text{NA}}(\phi) = \int_{-\infty}^0 \mathbb{P}_{\text{fix}}(\beta) \phi(\beta) d\beta, \quad (7)$$

$$= \int_{-\infty}^0 \frac{\beta}{1 - e^{-\beta}} \phi(\beta) d\beta, \quad (8)$$

$$= \int_{-\infty}^0 \frac{\beta}{1 - e^{-\beta}} (1 - p_b) f_{\Gamma}(-\beta; -\beta_d, b) d\beta. \quad (9)$$

$$(10)$$

Altogether, $\omega_A^{\text{polyDFE}}$ is given as:

$$\omega_A^{\text{polyDFE}} = d_N/d_S - \omega_{\text{NA}}(\phi), \quad (11)$$

$$= d_N/d_S - \int_{-\infty}^0 \frac{\beta}{1 - e^{-\beta}} \phi(\beta) d\beta. \quad (12)$$

Mutation-selection codon model at gene level ($\alpha=0.025$)

Figure S11:

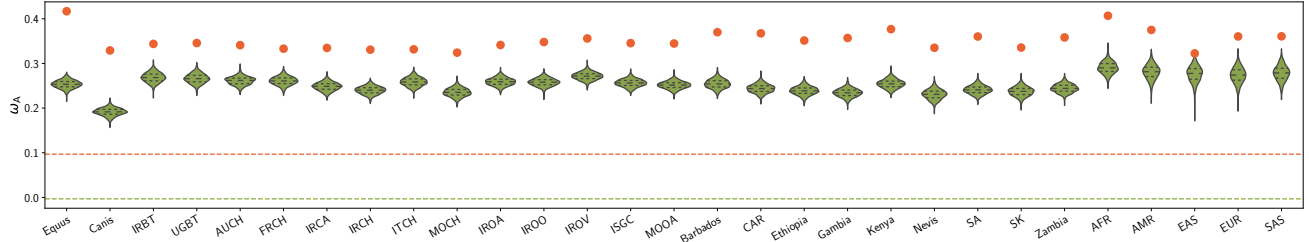


Table S11:

Population	Species	ω_A Adaptive	$\langle \omega_A \rangle$ Nearly-neutral	$\Delta\omega_A$	p_V	p_V^{adj}	$\frac{\Delta\omega_A}{\omega_A^{\text{Phy}}}$	π_S
Diverse (Equus)	Equus caballus	0.417	0.253	0.163	0.0	0.0*	1.702	0.00093
Diverse (Canis)	Canis familiaris	0.329	0.191	0.138	0.0	0.0*	1.335	0.001
Iran (IRBT)	Bos taurus	0.344	0.269	0.075	0.0	0.0*	0.748	0.003
Uganda (UGBT)	Bos taurus	0.346	0.266	0.080	0.0	0.0*	0.784	0.003
Australia (AUCH)	Capra hircus	0.341	0.261	0.080	0.0	0.0*	0.820	0.00099
France (FRCH)	Capra hircus	0.333	0.261	0.072	0.0	0.0*	0.744	0.00097
Iran (IRCA)	Capra aegagrus	0.335	0.248	0.086	0.0	0.0*	0.892	0.001
Iran (IRCH)	Capra hircus	0.331	0.240	0.091	0.0	0.0*	0.921	0.001
Italy (ITCH)	Capra hircus	0.332	0.259	0.073	0.0	0.0*	0.762	0.001
Morocco (MOCH)	Capra hircus	0.324	0.235	0.089	0.0	0.0*	0.886	0.001
Iran (IROA)	Ovis aries	0.341	0.259	0.082	0.0	0.0*	0.823	0.002
Iran (IROO)	Ovis orientalis	0.348	0.258	0.090	0.0	0.0*	0.901	0.003
Iran (IROV)	Ovis vignei	0.356	0.272	0.084	0.0	0.0*	0.860	0.002
Various (ISGC)	Ovis aries	0.346	0.256	0.089	0.0	0.0*	0.888	0.003
Morocco (MOOA)	Ovis aries	0.345	0.252	0.093	0.0	0.0*	0.921	0.002
Barbados	Chlorocebus sabaesus	0.370	0.254	0.116	0.0	0.0*	1.156	0.001
Central African Republic (CAR)	Chlorocebus sabaesus	0.367	0.244	0.124	0.0	0.0*	1.234	0.002
Ethiopia	Chlorocebus sabaesus	0.351	0.239	0.112	0.0	0.0*	1.126	0.002
Gambia	Chlorocebus sabaesus	0.357	0.234	0.123	0.0	0.0*	1.219	0.002
Kenya	Chlorocebus sabaesus	0.377	0.255	0.122	0.0	0.0*	1.245	0.001
Nevis	Chlorocebus sabaesus	0.335	0.231	0.104	0.0	0.0*	1.059	0.001
South Africa (SA)	Chlorocebus sabaesus	0.360	0.241	0.119	0.0	0.0*	1.184	0.002
Saint Kitts (SK)	Chlorocebus sabaesus	0.336	0.237	0.098	0.0	0.0*	0.983	0.001
Zambia	Chlorocebus sabaesus	0.358	0.244	0.114	0.0	0.0*	1.137	0.002
African (AFR)	Homo sapiens	0.407	0.290	0.116	0.0	0.0*	1.131	0.00071
Ad Mixed American (AMR)	Homo sapiens	0.375	0.281	0.094	0.0	0.0*	0.917	0.00056
East Asian (EAS)	Homo sapiens	0.323	0.276	0.046	0.0	0.0*	0.449	0.00051
European (EUR)	Homo sapiens	0.360	0.273	0.087	0.0	0.0*	0.847	0.00054
South Asian (SAS)	Homo sapiens	0.361	0.278	0.082	0.0	0.0*	0.805	0.00056

Mutation-selection codon model at site level ($\alpha=0.025$)

Figure S12:

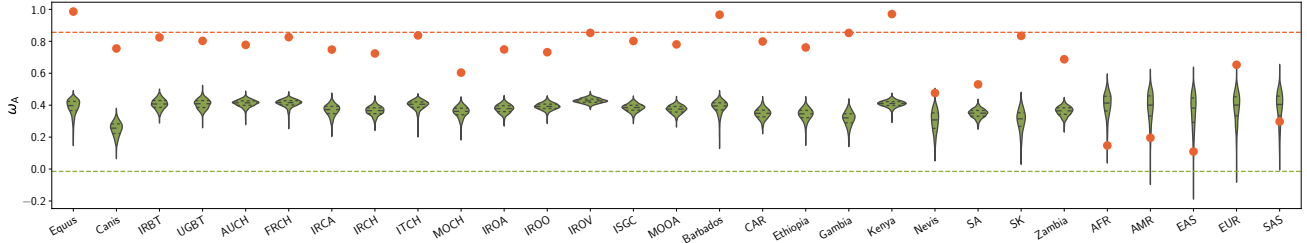


Table S12:

Population	Species	ω_A Adaptive	$\langle \omega_A \rangle$ Nearly-neutral	$\Delta\omega_A$	p_V	p_V^{adj}	$\frac{\Delta\omega_A}{\omega_A^{\text{PHY}}}$	π_S
Diverse (Equus)	Equus caballus	0.986	0.388	0.598	0.0	0.0*	0.688	0.00093
Diverse (Canis)	Canis familiaris	0.755	0.251	0.504	0.0	0.0*	0.575	0.001
Iran (IRBT)	Bos taurus	0.824	0.407	0.418	0.0	0.0*	0.480	0.003
Uganda (UGBT)	Bos taurus	0.803	0.407	0.396	0.0	0.0*	0.455	0.003
Australia (AUCH)	Capra hircus	0.778	0.412	0.366	0.0	0.0*	0.417	0.00099
France (FRCH)	Capra hircus	0.826	0.413	0.413	0.0	0.0*	0.472	0.00097
Iran (IRCA)	Capra aegagrus	0.748	0.368	0.380	0.0	0.0*	0.436	0.001
Iran (IRCH)	Capra hircus	0.724	0.364	0.360	0.0	0.0*	0.412	0.001
Italy (ITCH)	Capra hircus	0.837	0.401	0.436	0.0	0.0*	0.500	0.001
Morocco (MOCH)	Capra hircus	0.604	0.357	0.247	0.0	0.0*	0.282	0.001
Iran (IROA)	Ovis aries	0.749	0.378	0.371	0.0	0.0*	0.425	0.002
Iran (IROO)	Ovis orientalis	0.732	0.392	0.339	0.0	0.0*	0.390	0.003
Iran (IROV)	Ovis vignei	0.853	0.428	0.425	0.0	0.0*	0.489	0.002
Various (ISGC)	Ovis aries	0.802	0.384	0.418	0.0	0.0*	0.478	0.003
Morocco (MOOA)	Ovis aries	0.781	0.373	0.407	0.0	0.0*	0.466	0.002
Barbados	Chlorocebus sabaues	0.966	0.386	0.580	0.0	0.0*	0.668	0.001
Central African Republic (CAR)	Chlorocebus sabaues	0.799	0.347	0.452	0.0	0.0*	0.521	0.002
Ethiopia	Chlorocebus sabaues	0.762	0.343	0.419	0.0	0.0*	0.482	0.002
Gambia	Chlorocebus sabaues	0.852	0.316	0.536	0.0	0.0*	0.618	0.002
Kenya	Chlorocebus sabaues	0.971	0.410	0.561	0.0	0.0*	0.649	0.001
Nevis	Chlorocebus sabaues	0.476	0.300	0.176	0.0	0.0*	0.203	0.001
South Africa (SA)	Chlorocebus sabaues	0.530	0.348	0.182	0.0	0.0*	0.209	0.002
Saint Kitts (SK)	Chlorocebus sabaues	0.834	0.307	0.527	0.0	0.0*	0.607	0.001
Zambia	Chlorocebus sabaues	0.687	0.362	0.326	0.0	0.0*	0.375	0.002
African (AFR)	Homo sapiens	0.148	0.404	-0.256	0.995	1.000	-0.294	0.00071
Ad Mixed American (AMR)	Homo sapiens	0.196	0.388	-0.192	0.961	1.000	-0.220	0.00056
East Asian (EAS)	Homo sapiens	0.110	0.360	-0.250	0.977	1.000	-0.287	0.00051
European (EUR)	Homo sapiens	0.653	0.385	0.268	0.0	0.0*	0.307	0.00054
South Asian (SAS)	Homo sapiens	0.298	0.388	-0.090	0.840	1.000	-0.104	0.00056

- At the gene level, sets of genes supposedly under a nearly-neutral regime have an average value of $\omega_A^{\text{polyDFE}}$ (average across the replicates) in the range [0.19, 0.29] across the populations, while $\omega_A^{\text{polyDFE}}$ for genes under adaptation (at the phylogenetic scale) is in the range [0.32, 0.42] across the populations.
- At the site level, sets of sites supposedly under a nearly-neutral regime have an average value of $\omega_A^{\text{polyDFE}}$ (average across the replicates) in the range [0.25, 0.42] across the populations, while $\omega_A^{\text{polyDFE}}$ for genes under adaptation (at the phylogenetic scale) is in the range [0.11, 0.99] across the populations.

$\omega_A^{\text{polyDFE}}$ computed with polyDFE is higher than ω_A computed as the McDonald & Kreitman [5] statistic (figure 3 and table 1 in the main manuscript), suggesting that polyDFE has higher sensitivity to detect adaptation at the population-genetic scale. However, the genes and sites supposedly under a nearly-neutral regime have all values of $\omega_A^{\text{polyDFE}}$ greater than 0, suggesting that the higher sensitivity (true positive rate) also results in a lower specificity (true negative rate). Altogether, the statistical test for the enrichment of ω_A between the set of adaptive and nearly-neutral genes and sites gives similar results whether computed by polyDFE ($\omega_A^{\text{polyDFE}}$) or as McDonald & Kreitman [5] statistic.

6.2 PolyDFE model C - polymorphism data alone with $\beta > 0$

As in Tataru *et al.* [3], the rate of adaptation $\omega_A^{\text{polyDFE}}$ can also be estimated from the polymorphism data alone, computed as the average fixation probability $\mathbb{P}_{\text{fix}}(\beta)$ over the probability given the DFE ($\phi(\beta)$), only for the positively selected mutations ($\beta > 0$), as:

$$\omega_A^{\text{polyDFE}} = \int_0^{+\infty} \mathbb{P}_{\text{fix}}(\beta) \phi(\beta) d\beta, \quad (13)$$

$$= \int_0^{+\infty} \frac{\beta}{1 - e^{-\beta}} \phi(\beta) d\beta, \quad (14)$$

$$= \int_0^{+\infty} \frac{\beta}{1 - e^{-\beta}} p_b f_e(\beta; \beta_b) d\beta. \quad (15)$$

Mutation-selection codon model at gene level ($\alpha=0.025$)

Figure S13:

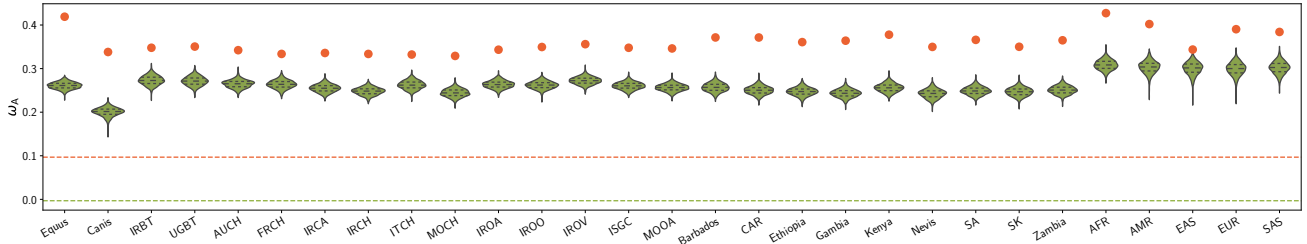


Table S13:

Population	Species	ω_A Adaptive	$\langle \omega_A \rangle$ Nearly-neutral	$\Delta\omega_A$	p_v	p_v^{adj}	$\frac{\Delta\omega_A}{\omega_A^{\text{poly}}}$	π_S
Diverse (Equus)	Equus caballus	0.419	0.261	0.158	0.0	0.0*	1.645	0.00093
Diverse (Canis)	Canis familiaris	0.338	0.201	0.138	0.0	0.0*	1.333	0.001
Iran (IRBT)	Bos taurus	0.348	0.273	0.075	0.0	0.0*	0.744	0.003
Uganda (UGBT)	Bos taurus	0.351	0.271	0.079	0.0	0.0*	0.779	0.003
Australia (AUCH)	Capra hircus	0.342	0.265	0.078	0.0	0.0*	0.799	0.00099
France (FRCH)	Capra hircus	0.334	0.264	0.070	0.0	0.0*	0.721	0.00097
Iran (IRCA)	Capra aegagrus	0.336	0.255	0.081	0.0	0.0*	0.837	0.001
Iran (IRCH)	Capra hircus	0.334	0.248	0.086	0.0	0.0*	0.866	0.001
Italy (ITCH)	Capra hircus	0.332	0.262	0.070	0.0	0.0*	0.730	0.001
Morocco (MOCH)	Capra hircus	0.329	0.244	0.085	0.0	0.0*	0.844	0.001
Iran (IROA)	Ovis aries	0.343	0.263	0.080	0.0	0.0*	0.799	0.002
Iran (IROO)	Ovis orientalis	0.350	0.262	0.087	0.0	0.0*	0.877	0.003
Iran (IROV)	Ovis vignei	0.356	0.272	0.084	0.0	0.0*	0.853	0.002
Various (ISGC)	Ovis aries	0.348	0.260	0.087	0.0	0.0*	0.868	0.003
Morocco (MOOA)	Ovis aries	0.346	0.256	0.090	0.0	0.0*	0.888	0.002
Barbados	Chlorocebus sabaesus	0.371	0.257	0.114	0.0	0.0*	1.145	0.001
Central African Republic (CAR)	Chlorocebus sabaesus	0.371	0.250	0.121	0.0	0.0*	1.208	0.002
Ethiopia	Chlorocebus sabaesus	0.361	0.247	0.114	0.0	0.0*	1.137	0.002
Gambia	Chlorocebus sabaesus	0.364	0.243	0.121	0.0	0.0*	1.199	0.002
Kenya	Chlorocebus sabaesus	0.378	0.256	0.122	0.0	0.0*	1.240	0.001
Nevis	Chlorocebus sabaesus	0.350	0.242	0.107	0.0	0.0*	1.087	0.001
South Africa (SA)	Chlorocebus sabaesus	0.366	0.249	0.117	0.0	0.0*	1.160	0.002
Saint Kitts (SK)	Chlorocebus sabaesus	0.350	0.247	0.103	0.0	0.0*	1.033	0.001
Zambia	Chlorocebus sabaesus	0.365	0.251	0.114	0.0	0.0*	1.139	0.002
African (AFR)	Homo sapiens	0.427	0.309	0.119	0.0	0.0*	1.154	0.00071
Ad Mixed American (AMR)	Homo sapiens	0.402	0.303	0.099	0.0	0.0*	0.963	0.00056
East Asian (EAS)	Homo sapiens	0.344	0.300	0.043	0.0	0.0*	0.421	0.00051
European (EUR)	Homo sapiens	0.390	0.299	0.091	0.0	0.0*	0.886	0.00054
South Asian (SAS)	Homo sapiens	0.384	0.302	0.082	0.0	0.0*	0.799	0.00056

Mutation-selection codon model at site level ($\alpha=0.025$)

Figure S14:

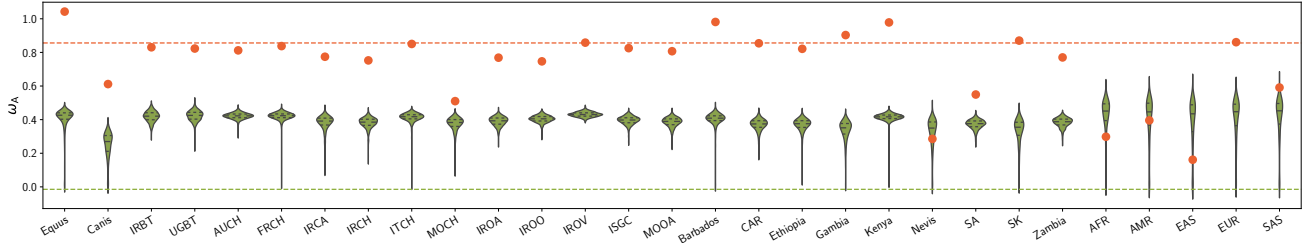


Table S14:

Population	Species	ω_A Adaptive	$\langle \omega_A \rangle$ Nearly-neutral	$\Delta \omega_A$	p_V	p_V^{adj}	$\frac{\Delta \omega_A}{\omega_A^{\text{phy}}}$	π_S
Diverse (Equus)	Equus caballus	1.043	0.407	0.636	0.0	0.0*	0.732	0.00093
Diverse (Canis)	Canis familiaris	0.612	0.249	0.363	0.0	0.0*	0.414	0.001
Iran (IRBT)	Bos taurus	0.830	0.418	0.412	0.0	0.0*	0.474	0.003
Uganda (UGBT)	Bos taurus	0.823	0.423	0.400	0.0	0.0*	0.461	0.003
Australia (AUCH)	Capra hircus	0.812	0.422	0.390	0.0	0.0*	0.446	0.00099
France (FRCH)	Capra hircus	0.838	0.419	0.418	0.0	0.0*	0.478	0.00097
Iran (IRCA)	Capra aegagrus	0.774	0.382	0.392	0.0	0.0*	0.450	0.001
Iran (IRCH)	Capra hircus	0.752	0.381	0.372	0.0	0.0*	0.425	0.001
Italy (ITCH)	Capra hircus	0.850	0.412	0.438	0.0	0.0*	0.502	0.001
Morocco (MOCH)	Capra hircus	0.510	0.374	0.136	0.0	0.0*	0.156	0.001
Iran (IROA)	Ovis aries	0.769	0.390	0.379	0.0	0.0*	0.434	0.002
Iran (IROO)	Ovis orientalis	0.747	0.404	0.343	0.0	0.0*	0.394	0.003
Iran (IROV)	Ovis vignei	0.858	0.431	0.427	0.0	0.0*	0.492	0.002
Various (ISGC)	Ovis aries	0.825	0.395	0.430	0.0	0.0*	0.492	0.003
Morocco (MOOA)	Ovis aries	0.807	0.385	0.422	0.0	0.0*	0.483	0.002
Barbados	Chlorocebus sabaues	0.981	0.399	0.582	0.0	0.0*	0.670	0.001
Central African Republic (CAR)	Chlorocebus sabaues	0.854	0.370	0.484	0.0	0.0*	0.558	0.002
Ethiopia	Chlorocebus sabaues	0.821	0.370	0.452	0.0	0.0*	0.520	0.002
Gambia	Chlorocebus sabaues	0.903	0.338	0.565	0.0	0.0*	0.651	0.002
Kenya	Chlorocebus sabaues	0.978	0.416	0.562	0.0	0.0*	0.650	0.001
Nevis	Chlorocebus sabaues	0.286	0.326	-0.040	0.771	1.000	-0.047	0.001
South Africa (SA)	Chlorocebus sabaues	0.549	0.373	0.177	0.0	0.0*	0.203	0.002
Saint Kitts (SK)	Chlorocebus sabaues	0.870	0.332	0.538	0.0	0.0*	0.620	0.001
Zambia	Chlorocebus sabaues	0.770	0.384	0.386	0.0	0.0*	0.445	0.002
African (AFR)	Homo sapiens	0.298	0.425	-0.127	0.898	1.000	-0.146	0.00071
Ad Mixed American (AMR)	Homo sapiens	0.396	0.406	-0.010	0.681	1.000	-0.011	0.00056
East Asian (EAS)	Homo sapiens	0.161	0.382	-0.221	0.882	1.000	-0.253	0.00051
European (EUR)	Homo sapiens	0.861	0.407	0.454	0.0	0.0*	0.521	0.00054
South Asian (SAS)	Homo sapiens	0.591	0.409	0.182	0.001	0.005*	0.208	0.00056

- At the gene level, sets of genes supposedly under a nearly-neutral regime have an average value of $\omega_A^{\text{polyDFE}}$ (average across the replicates) in the range [0.20, 0.31] across the populations, while $\omega_A^{\text{polyDFE}}$ for genes under adaptation (at the phylogenetic scale) is in the range [0.32, 0.43] across the populations.
- At the site level, sets of sites supposedly under a nearly-neutral regime have an average value of $\omega_A^{\text{polyDFE}}$ (average across the replicates) in the range [0.24, 0.44] across the populations, while $\omega_A^{\text{polyDFE}}$ for genes under adaptation (at the phylogenetic scale) is in the range [0.16, 1.04] across the populations.

The estimation of $\omega_A^{\text{polyDFE}}$ computed with polyDFE using polymorphism data alone is quite consistent with the estimation combining polymorphism and divergence (previous section). However, we higher variance in the estimation (violin plots are more extended for the set of nearly-neutral replicates, particularly noticeable for sites), reducing the statistical power for the enrichment test of $\omega_A^{\text{polyDFE}}$ between the set of adaptive and nearly-neutral genes and sites.

6.3 PolyDFE model C - polymorphism data alone with $\beta > 5$

The definition for a positively selected mutation by the criterion $\beta > 0$ is also open to interpretation, and the integration limit can be set to a strictly positive value (e.g. 1, 3 or 5) instead of 0 [3, 6]. The reasoning is that mutations with a positive selection coefficient that is not very large are not necessarily advantageous mutations. In Galtier [6], the threshold $\beta > 5$ is used and the rate of adaptation is thus:

$$\omega_A^{\text{polyDFE}} = \int_5^{+\infty} \frac{\beta}{1 - e^{-\beta}} p_b f_e(\beta; \beta_b) d\beta. \quad (16)$$

Mutation-selection codon model at gene level ($\alpha=0.025$)

Figure S15:

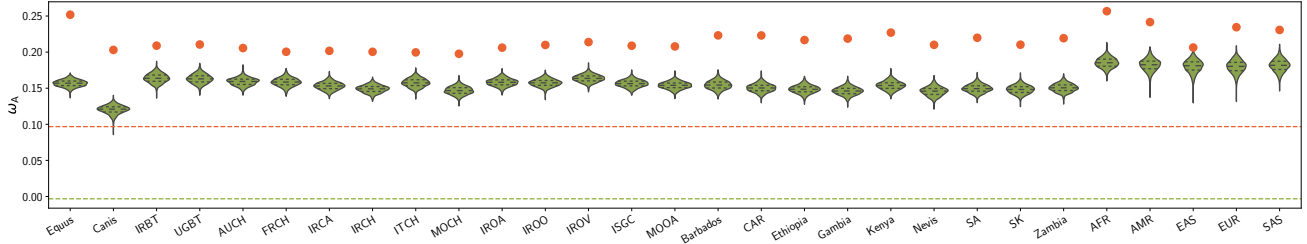


Table S15:

Population	Species	ω_A Adaptive	$\langle \omega_A \rangle$ Nearly-neutral	$\Delta \omega_A$	p_v	p_v^{adj}	$\frac{\Delta \omega_A}{\omega_{\text{phy}}}$	π_S
Diverse (Equus)	Equus caballus	0.252	0.157	0.095	0.0	0.0*	0.989	0.00093
Diverse (Canis)	Canis familiaris	0.203	0.120	0.083	0.0	0.0*	0.802	0.001
Iran (IRBT)	Bos taurus	0.209	0.164	0.045	0.0	0.0*	0.447	0.003
Uganda (UGBT)	Bos taurus	0.211	0.163	0.048	0.0	0.0*	0.468	0.003
Australia (AUCH)	Capra hircus	0.206	0.159	0.047	0.0	0.0*	0.480	0.00099
France (FRCH)	Capra hircus	0.200	0.158	0.042	0.0	0.0*	0.433	0.00097
Iran (IRCA)	Capra aegagrus	0.202	0.153	0.049	0.0	0.0*	0.503	0.001
Iran (IRCH)	Capra hircus	0.200	0.149	0.051	0.0	0.0*	0.521	0.001
Italy (ITCH)	Capra hircus	0.200	0.158	0.042	0.0	0.0*	0.439	0.001
Morocco (MOCH)	Capra hircus	0.198	0.147	0.051	0.0	0.0*	0.507	0.001
Iran (IROA)	Ovis aries	0.206	0.158	0.048	0.0	0.0*	0.480	0.002
Iran (IROO)	Ovis orientalis	0.210	0.157	0.053	0.0	0.0*	0.527	0.003
Iran (IROV)	Ovis vignei	0.214	0.164	0.050	0.0	0.0*	0.513	0.002
Various (ISGC)	Ovis aries	0.209	0.156	0.052	0.0	0.0*	0.522	0.003
Morocco (MOOA)	Ovis aries	0.208	0.154	0.054	0.0	0.0*	0.534	0.002
Barbados	Chlorocebus sabaesus	0.223	0.154	0.069	0.0	0.0*	0.688	0.001
Central African Republic (CAR)	Chlorocebus sabaesus	0.223	0.150	0.073	0.0	0.0*	0.726	0.002
Ethiopia	Chlorocebus sabaesus	0.217	0.148	0.068	0.0	0.0*	0.683	0.002
Gambia	Chlorocebus sabaesus	0.219	0.146	0.073	0.0	0.0*	0.721	0.002
Kenya	Chlorocebus sabaesus	0.227	0.154	0.073	0.0	0.0*	0.745	0.001
Nevis	Chlorocebus sabaesus	0.210	0.146	0.065	0.0	0.0*	0.654	0.001
South Africa (SA)	Chlorocebus sabaesus	0.220	0.150	0.070	0.0	0.0*	0.698	0.002
Saint Kitts (SK)	Chlorocebus sabaesus	0.210	0.148	0.062	0.0	0.0*	0.621	0.001
Zambia	Chlorocebus sabaesus	0.219	0.151	0.069	0.0	0.0*	0.684	0.002
African (AFR)	Homo sapiens	0.257	0.185	0.071	0.0	0.0*	0.693	0.00071
Ad Mixed American (AMR)	Homo sapiens	0.242	0.182	0.059	0.0	0.0*	0.578	0.00056
East Asian (EAS)	Homo sapiens	0.206	0.180	0.026	0.0	0.0*	0.252	0.00051
European (EUR)	Homo sapiens	0.234	0.180	0.055	0.0	0.0*	0.532	0.00054
South Asian (SAS)	Homo sapiens	0.231	0.182	0.049	0.0	0.0*	0.480	0.00056

Mutation-selection codon model at site level ($\alpha=0.025$)

Figure S16:

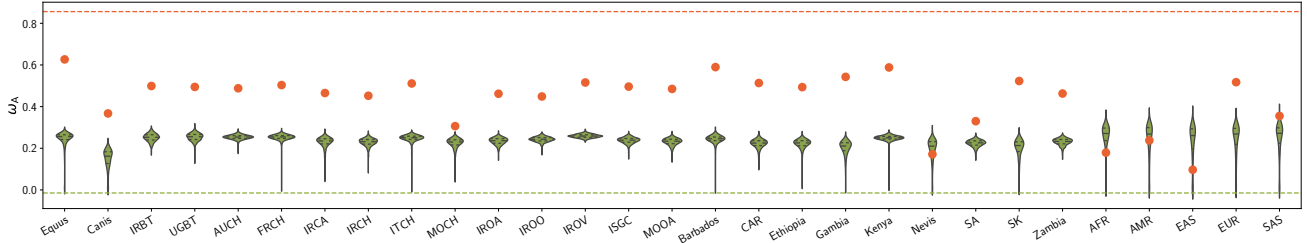


Table S16:

Population	Species	ω_A Adaptive	$\langle \omega_A \rangle$ Nearly-neutral	$\Delta \omega_A$	p_V	p_V^{adj}	$\frac{\Delta \omega_A}{\omega_A^{\text{phy}}}$	π_S
Diverse (Equus)	Equus caballus	0.627	0.244	0.382	0.0	0.0*	0.440	0.00093
Diverse (Canis)	Canis familiaris	0.367	0.149	0.218	0.0	0.0*	0.249	0.001
Iran (IRBT)	Bos taurus	0.499	0.251	0.248	0.0	0.0*	0.285	0.003
Uganda (UGBT)	Bos taurus	0.495	0.254	0.241	0.0	0.0*	0.277	0.003
Australia (AUCH)	Capra hircus	0.488	0.253	0.235	0.0	0.0*	0.268	0.00099
France (FRCH)	Capra hircus	0.503	0.252	0.251	0.0	0.0*	0.287	0.00097
Iran (IRCA)	Capra aegagrus	0.465	0.229	0.236	0.0	0.0*	0.270	0.001
Iran (IRCH)	Capra hircus	0.452	0.229	0.223	0.0	0.0*	0.256	0.001
Italy (ITCH)	Capra hircus	0.511	0.248	0.263	0.0	0.0*	0.302	0.001
Morocco (MOCH)	Capra hircus	0.306	0.224	0.082	0.0	0.0*	0.094	0.001
Iran (IROA)	Ovis aries	0.462	0.234	0.228	0.0	0.0*	0.261	0.002
Iran (IROO)	Ovis orientalis	0.449	0.243	0.206	0.0	0.0*	0.237	0.003
Iran (IROV)	Ovis vignei	0.516	0.259	0.257	0.0	0.0*	0.296	0.002
Various (ISGC)	Ovis aries	0.496	0.237	0.259	0.0	0.0*	0.296	0.003
Morocco (MOOA)	Ovis aries	0.485	0.231	0.254	0.0	0.0*	0.290	0.002
Barbados	Chlorocebus sabaesus	0.590	0.240	0.350	0.0	0.0*	0.403	0.001
Central African Republic (CAR)	Chlorocebus sabaesus	0.513	0.222	0.291	0.0	0.0*	0.335	0.002
Ethiopia	Chlorocebus sabaesus	0.494	0.222	0.271	0.0	0.0*	0.313	0.002
Gambia	Chlorocebus sabaesus	0.543	0.203	0.340	0.0	0.0*	0.392	0.002
Kenya	Chlorocebus sabaesus	0.588	0.250	0.338	0.0	0.0*	0.391	0.001
Nevis	Chlorocebus sabaesus	0.171	0.196	-0.024	0.773	1.000	-0.028	0.001
South Africa (SA)	Chlorocebus sabaesus	0.330	0.224	0.106	0.0	0.0*	0.122	0.002
Saint Kitts (SK)	Chlorocebus sabaesus	0.523	0.199	0.323	0.0	0.0*	0.373	0.001
Zambia	Chlorocebus sabaesus	0.463	0.230	0.232	0.0	0.0*	0.267	0.002
African (AFR)	Homo sapiens	0.179	0.255	-0.076	0.898	1.000	-0.088	0.00071
Ad Mixed American (AMR)	Homo sapiens	0.238	0.244	-0.006	0.681	1.000	-0.007	0.00056
East Asian (EAS)	Homo sapiens	0.097	0.230	-0.133	0.882	1.000	-0.152	0.00051
European (EUR)	Homo sapiens	0.517	0.244	0.273	0.0	0.0*	0.313	0.00054
South Asian (SAS)	Homo sapiens	0.355	0.246	0.109	0.001	0.005*	0.125	0.00056

- At the gene level, sets of genes supposedly under a nearly-neutral regime have an average value of $\omega_A^{\text{polyDFE}}$ (average across the replicates) in the range $[0.12, 0.19]$ across the populations, while $\omega_A^{\text{polyDFE}}$ for genes under adaptation (at the phylogenetic scale) is in the range $[0.20, 0.26]$ across the populations.
- At the site level, sets of sites supposedly under a nearly-neutral regime have an average value of $\omega_A^{\text{polyDFE}}$ (average across the replicates) in the range $[0.14, 0.26]$ across the populations, while $\omega_A^{\text{polyDFE}}$ for genes under adaptation (at the phylogenetic scale) is in the range $[0.09, 0.63]$ across the populations.

The estimation of $\omega_A^{\text{polyDFE}}$ computed with polyDFE using polymorphism data alone and with a bound of $\beta > 5$ to consider a mutation as adaptive[6] is lower than $\omega_A^{\text{polyDFE}}$ computed with a bound of $\beta > 0$ [3]. However, the genes and sites supposedly under a nearly-neutral regime still have values of $\omega_A^{\text{polyDFE}}$ greater than 0, suggesting that $\omega_A^{\text{polyDFE}}$ still has a lower specificity than the McDonald & Kreitman [5] statistic.

6.4 PolyDFE model D - including divergence

Again, the rate of adaptation $\omega_A^{\text{polyDFE}}$ is computed as the difference between the total rate of evolution $\omega = d_N/d_S$ obtained from divergence data and the rate of non-adaptive evolution ($\omega_{\text{NA}}(\phi)$) obtained from polymorphism data. Also, $\omega_{\text{NA}}(\phi)$ is computed as the average fixation probability of mutations ($\mathbb{P}_{\text{fix}}(\beta)$) over the probability distribution given by the DFE $\phi(\beta)$, taken only for the negatively selected mutations ($\beta < 0$) as:

$$\omega_{\text{NA}}(\phi) = \sum_{i=1}^K \mathbb{1}_{]-\infty, 0]}(\beta_i) \mathbb{P}_{\text{fix}}(\beta_i) p_i, \quad (17)$$

$$= \sum_{i=1}^K \mathbb{1}_{]-\infty, 0]}(\beta_i) \frac{\beta_i}{1 - e^{-\beta_i}} p_i, \quad (18)$$

where $\mathbb{1}_{]-\infty, 0]}(\beta)$ is the indicator function:

$$\mathbb{1}_{]-\infty, 0]}(\beta) = \begin{cases} 1 & \text{if } \beta \leq 0, \\ 0 & \text{if } \beta > 0. \end{cases} \quad (19)$$

Altogether, $\omega_A^{\text{polyDFE}}$ is given as:

$$\omega_A^{\text{polyDFE}} = d_N/d_S - \sum_{i=1}^K \mathbb{1}_{]-\infty, 0]}(\beta_i) \frac{\beta_i}{1 - e^{-\beta_i}} p_i. \quad (20)$$

Mutation-selection codon model at gene level ($\alpha=0.025$)

Figure S17:

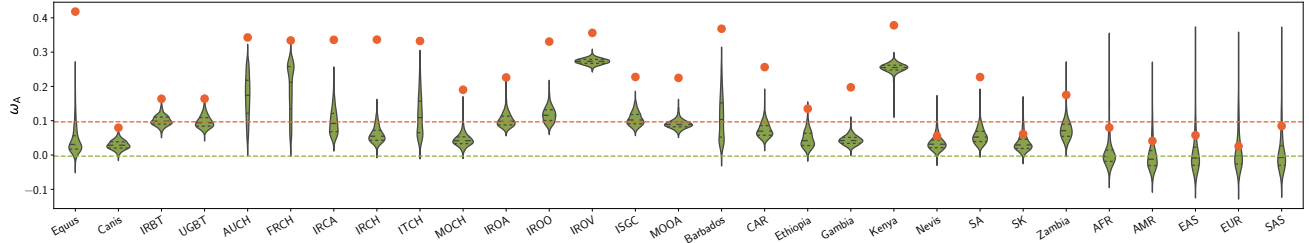


Table S17:

Population	Species	ω_A Adaptive	$\langle \omega_A \rangle$ Nearly-neutral	$\Delta\omega_A$	p_v	p_v^{adj}	$\frac{\Delta\omega_A}{\omega^{\text{phy}}_A}$	π_S
Diverse (Equus)	Equus caballus	0.418	0.043	0.375	0.0	0.0*	3.907	0.00093
Diverse (Canis)	Canis familiaris	0.080	0.029	0.050	0.0	0.0*	0.488	0.001
Iran (IRBT)	Bos taurus	0.164	0.101	0.063	0.003	0.027*	0.627	0.003
Uganda (UGBT)	Bos taurus	0.164	0.098	0.066	0.001	0.011*	0.651	0.003
Australia (AUCH)	Capra hircus	0.343	0.170	0.173	0.0	0.0*	1.782	0.00099
France (FRCH)	Capra hircus	0.334	0.193	0.141	0.0	0.0*	1.455	0.00097
Iran (IRCA)	Capra aegagrus	0.336	0.097	0.238	0.0	0.0*	2.464	0.001
Iran (IRCH)	Capra hircus	0.336	0.060	0.277	0.0	0.0*	2.800	0.001
Italy (ITCH)	Capra hircus	0.332	0.116	0.216	0.0	0.0*	2.256	0.001
Morocco (MOCH)	Capra hircus	0.190	0.045	0.146	0.0	0.0*	1.453	0.001
Iran (IROA)	Ovis aries	0.226	0.102	0.124	0.0	0.0*	1.237	0.002
Iran (IROO)	Ovis orientalis	0.331	0.117	0.213	0.0	0.0*	2.143	0.003
Iran (IROV)	Ovis vignei	0.356	0.273	0.083	0.0	0.0*	0.848	0.002
Various (ISGC)	Ovis aries	0.228	0.105	0.122	0.0	0.0*	1.214	0.003
Morocco (MOOA)	Ovis aries	0.225	0.090	0.135	0.0	0.0*	1.331	0.002
Barbados	Chlorocebus sabaeus	0.368	0.109	0.260	0.0	0.0*	2.596	0.001
Central African Republic (CAR)	Chlorocebus sabaeus	0.256	0.073	0.183	0.0	0.0*	1.827	0.002
Ethiopia	Chlorocebus sabaeus	0.135	0.047	0.088	0.002	0.020*	0.885	0.002
Gambia	Chlorocebus sabaeus	0.198	0.043	0.154	0.0	0.0*	1.533	0.002
Kenya	Chlorocebus sabaeus	0.378	0.253	0.125	0.0	0.0*	1.278	0.001
Nevis	Chlorocebus sabaeus	0.055	0.035	0.020	0.136	0.618	0.206	0.001
South Africa (SA)	Chlorocebus sabaeus	0.227	0.056	0.172	0.0	0.0*	1.704	0.002
Saint Kitts (SK)	Chlorocebus sabaeus	0.061	0.035	0.026	0.108	0.618	0.265	0.001
Zambia	Chlorocebus sabaeus	0.175	0.073	0.102	0.007	0.056	1.016	0.002
African (AFR)	Homo sapiens	0.080	0.003	0.077	0.035	0.245	0.747	0.00071
Ad Mixed American (AMR)	Homo sapiens	0.041	-0.003	0.045	0.119	0.618	0.435	0.00056
East Asian (EAS)	Homo sapiens	0.058	0.007	0.051	0.142	0.618	0.496	0.00051
European (EUR)	Homo sapiens	0.026	0.014	0.011	0.289	0.618	0.109	0.00054
South Asian (SAS)	Homo sapiens	0.085	0.008	0.076	0.103	0.618	0.744	0.00056

Mutation-selection codon model at site level ($\alpha=0.025$)

Figure S18:

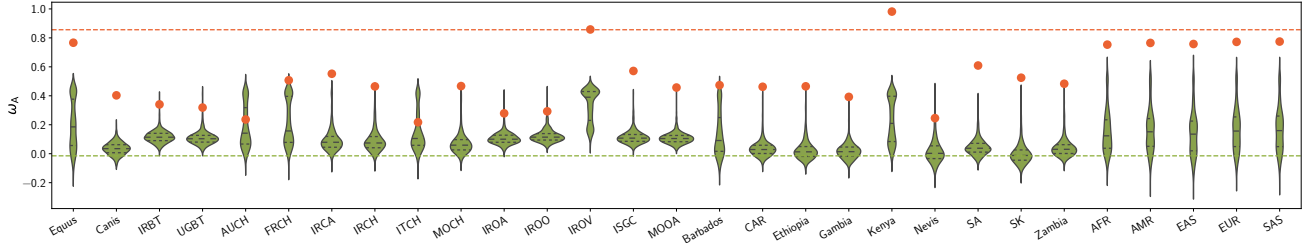


Table S18:

Population	Species	ω_A Adaptive	$\langle \omega_A \rangle$ Nearly-neutral	$\Delta\omega_A$	p_v	p_v^{adj}	$\frac{\Delta\omega_A}{\omega_A^{\text{phy}}}$	π_S
Diverse (Equus)	Equus caballus	0.767	0.202	0.565	0.0	0.0*	0.650	0.00093
Diverse (Canis)	Canis familiaris	0.403	0.035	0.368	0.0	0.0*	0.420	0.001
Iran (IRBT)	Bos taurus	0.340	0.117	0.223	0.002	0.014*	0.257	0.003
Uganda (UGBT)	Bos taurus	0.319	0.110	0.208	0.011	0.050	0.240	0.003
Australia (AUCH)	Capra hircus	0.236	0.188	0.049	0.352	0.498	0.056	0.00099
France (FRCH)	Capra hircus	0.507	0.213	0.295	0.0	0.0*	0.337	0.00097
Iran (IRCA)	Capra aegagrus	0.552	0.096	0.456	0.0	0.0*	0.523	0.001
Iran (IRCH)	Capra hircus	0.465	0.092	0.373	0.0	0.0*	0.427	0.001
Italy (ITCH)	Capra hircus	0.217	0.149	0.068	0.249	0.498	0.078	0.001
Morocco (MOCH)	Capra hircus	0.467	0.074	0.393	0.0	0.0*	0.450	0.001
Iran (IROA)	Ovis aries	0.279	0.107	0.172	0.010	0.050	0.197	0.002
Iran (IROO)	Ovis orientalis	0.293	0.123	0.170	0.008	0.048*	0.195	0.003
Iran (IROV)	Ovis vignei	0.858	0.334	0.524	0.0	0.0*	0.603	0.002
Various (ISGC)	Ovis aries	0.572	0.114	0.457	0.0	0.0*	0.523	0.003
Morocco (MOOA)	Ovis aries	0.457	0.108	0.349	0.0	0.0*	0.399	0.002
Barbados	Chlorocebus sabaeus	0.474	0.137	0.337	0.0	0.0*	0.388	0.001
Central African Republic (CAR)	Chlorocebus sabaeus	0.462	0.037	0.426	0.0	0.0*	0.490	0.002
Ethiopia	Chlorocebus sabaeus	0.465	0.025	0.440	0.0	0.0*	0.507	0.002
Gambia	Chlorocebus sabaeus	0.392	0.019	0.373	0.0	0.0*	0.430	0.002
Kenya	Chlorocebus sabaeus	0.982	0.229	0.753	0.0	0.0*	0.871	0.001
Nevis	Chlorocebus sabaeus	0.246	0.021	0.225	0.034	0.102	0.260	0.001
South Africa (SA)	Chlorocebus sabaeus	0.609	0.048	0.562	0.0	0.0*	0.645	0.002
Saint Kitts (SK)	Chlorocebus sabaeus	0.525	0.001	0.524	0.0	0.0*	0.603	0.001
Zambia	Chlorocebus sabaeus	0.483	0.043	0.440	0.0	0.0*	0.507	0.002
African (AFR)	Homo sapiens	0.753	0.151	0.602	0.0	0.0*	0.690	0.00071
Ad Mixed American (AMR)	Homo sapiens	0.765	0.162	0.603	0.0	0.0*	0.691	0.00056
East Asian (EAS)	Homo sapiens	0.758	0.140	0.618	0.0	0.0*	0.709	0.00051
European (EUR)	Homo sapiens	0.772	0.165	0.607	0.0	0.0*	0.696	0.00054
South Asian (SAS)	Homo sapiens	0.775	0.168	0.607	0.0	0.0*	0.697	0.00056

- At the gene level, $\omega_A^{\text{polyDFE}}$ for nearly-neutral genes is the range $[-0.01, 0.27]$, while $\omega_A^{\text{polyDFE}}$ for genes under adaptation (at the phylogenetic scale) is in the range $[0.04, 42]$.
- At the site level, $\omega_A^{\text{polyDFE}}$ for nearly-neutral sites is the range $[0.0, 0.34]$, while $\omega_A^{\text{polyDFE}}$ for sites under adaptation (at the phylogenetic scale) is in the range $[0.40, 0.98]$.

The estimation of $\omega_A^{\text{polyDFE}}$ computed with polyDFE using polymorphism and divergence data with either a the model C (continuous DFE) or D (discrete DFE) are quite different in absolute value. The underlying assumption for the mathematical constrains on the DFE thus have a large impact on the estimation of $\omega_A^{\text{polyDFE}}$ while the true underlying DFE is unknown.

7 References

1. Eyre-Walker, A., Woolfit, M. & Phelps, T. The Distribution of Fitness Effects of New Deleterious Amino Acid Mutations in Humans. *Genetics* **173**, 891–900 (2006).
2. Eyre-Walker, A. & Keightley, P. D. Estimating the Rate of Adaptive Molecular Evolution in the Presence of Slightly Deleterious Mutations and Population Size Change. *Molecular Biology and Evolution* **26**, 2097–2108 (2009).
3. Tataru, P., Mollion, M., Glémin, S. & Bataillon, T. Inference of Distribution of Fitness Effects and Proportion of Adaptive Substitutions from Polymorphism Data. *Genetics* **207**, 1103–1119 (2017).
4. Tataru, P. & Bataillon, T. *polyDFE: Inferring the Distribution of Fitness Effects and Properties of Beneficial Mutations from Polymorphism Data* in *Methods in Molecular Biology* 125–146 (Humana Press Inc., 2020).
5. McDonald, J. H. & Kreitman, M. Adaptive Protein Evolution at Adh Locus in *Drosophila*. *Nature* **351**, 652–654 (1991).
6. Galtier, N. Adaptive Protein Evolution in Animals and the Effective Population Size Hypothesis. *PLoS Genetics* **12**, e1005774 (2016).